DOE/PC/94210--T5

Pressure Fluctuations as a Diagnostic Tool for Fluidized Beds

Technical Progress Report for the Period
October 1, 1995 - December 30, 1995

Principal Investigator: Robert C. Brown
Research Assistant: Ethan Brue

Iowa State University
Ames, IA 50011

Work Performed Under Grant
No. DE-FG22-94PC94210

Date Transmitted: January 15, 1996

Prepared for: U.S. Department of Energy
Pittsburgh Energy Technology Center
Pittsburgh, PA

MASTER

DISTRIBUTION OF THIS DOCUMENT IS UNLIMITED

Pressure Fluctuations as a Diagnostic Tool for Fluidized Beds

Technical Progress Report for the Period
October 1, 1995 - December 30, 1995

Principal Investigator: Robert C. Brown
Research Assistant: Ethan Brue
Iowa State University
Ames, IA 50011

Abstract

Experimentation was conducted to determine the nature of bubbling fluidized bed (BFB) pressure fluctuations. The goal of the experiments was to explain the physical phenomena that governs the structure of pressure fluctuations. A study of the effect of the differential pressure tap spacing was conducted. The results confirmed the hypothesis that spatial aliasing can significantly distort expected fluctuation structure. The behavior of bubbling bed fluctuations was compared to previously published theories that predicted the natural frequency of incipiently fluidized beds. A modified theory was derived for fluidized systems which better predicts the observed frequency in shallow fluidized beds. This theory not only predicts the natural frequency of bed oscillations, but also explains the second order system behavior observed in bubbling fluidized bed Bode plots. The effect of bubble coalescence in deep beds acts both to decrease the frequency of bed oscillations and to complicate the observed frequency response with multiple peaks.

DISCLAIMER

This report was prepared as an account of work sponsored by an agency of the United States Government. Neither the United States Government nor any agency thereof, nor any of their employees, makes any warranty, express or implied, or assumes any legal liability or responsibility for the accuracy, completeness, or usefulness of any information, apparatus, product, or process disclosed, or represents that its use would not infringe privately owned rights. Reference herein to any specific commercial product, process, or service by trade name, trademark, manufacturer, or otherwise does not necessarily constitute or imply its endorsement, recommendation, or favoring by the United States Government or any agency thereof. The views and opinions of authors expressed herein do not necessarily state or reflect those of the United States Government or any agency thereof.

Pressure Fluctuations as a Diagnostic Tool for Fluidized Beds

Robert C. Brown and Ethan Brue

Objective

The purpose of this project is to investigate the origin of pressure fluctuations in fluidized bed systems. The study will asses the potential for using pressure fluctuations as an indicator of fluidized bed hydrodynamics in both laboratory scale cold-models and industrial scale boilers.

Progress

Motivation for Bubbling Bed Experimentation

The primary goal of this research is to study the nature of pressure fluctuations in circulating fluidized beds in order to asses how they can be used as a design tool (e.g. model scale-up) or diagnostic tool (e.g. boiler control) in industrial scale CFB combustors. In order to achieve this objective, it is necessary to have an adequate understanding of bubbling fluidized bed pressure fluctuations prior to studying similar fluctuations in CFBs for a number of reasons. First, the majority of previous research on this subject of fluidized bed fluctuations, has been conducted in bubbling fluidized beds. This body of published data and proposed theories provides a basis for comparison to our experimental results and subsequent hypotheses. Secondly, there are similarities in the structure of pressure fluctuations in bubbling fluidized beds and circulating fluidized beds. The fluctuations in the lower dense region of the CFB exhibit a similar frequency response profile as those observed in bubbling fluidized beds. Also, oscillatory second order system dynamics are observed in the fluctuation structure of all fluidization systems. Finally, fluidized bed similitude relations were first applied to bubbling beds and then extended to CFBs. Before the relations for CFB similitude can be validated using pressure fluctuations, the validity of using bubbling bed fluctuations to verify the achievement of BFB similitude must be addressed.

Despite the wealth of published research dealing with bubbling fluidized bed fluctuations, there is still no consensus as to the phenomena that governs pressure fluctuations. This fundamental question is a difficult one for a number of reasons. First of all, experimental data suggests that multiple phenomena acting simultaneously may be responsible for fluctuations in

fluidized bed systems. This being the case, the problem is not that previous studies have derived entirely incorrect theories for the appearance of periodic behavior in fluidized bed systems, but rather that they have composed an incomplete picture of a more complex system. Fluidized bed systems cannot always be characterized by a single frequency observed in the frequency spectrum. The characteristic frequency (or frequencies) of pressure fluctuations is not observed as a well defined single peak in the frequency response plots. Spectral analysis of fluidized bed fluctuations typically yields a broad distribution of frequencies centered around a dominant frequency. Therefore, any quantitative description of the fluctuation structure inherently contains a great deal of uncertainty. When multiple frequency phenomena are observed, this quantitative assessment becomes even more difficult. In addition to the complexity of the fluctuation signal, the configuration of the pressure measurement system plays a significant part in the information that can be obtained from pressure fluctuation measurements.

Measurement of Pressure Fluctuations in BFB Systems

As shown by Davidson for bubbling beds [1] and by Brue for circulating beds [2], differential pressure measurements and absolute pressure measurements can yield distinctly different periodic structure. The differential measurement typically reveals a dominant frequency in the spectrum that is at a higher frequency than the dominant frequency measured by absolute pressure measurement. While the differential pressure is a function of the fluctuations in the voidage between two pressure taps, absolute pressure measurements record the pressure drop from the tap position to the upper bed surface. Consequently, an absolute pressure measurement will sense a change in pressure as the amount of material above the point of measurement changes. The absolute measurement could be considered a differential pressure measurement with the upper tap positioned at the bed surface (assuming a non-pressurized BFB). Consequently, the difference between the resulting absolute and differential signals is essentially a difference arising from an increased tap spacing, which will be discussed in detail later.

As long as the measurement configuration remains the same (i.e. differential or absolute), the position of the observed frequency will not vary as the elevation of the pressure fluctuation measurement changes within the bed. This does not mean that the relative magnitude of each dominant frequency observed will not change. Figures 1 and 2 compare the frequency spectrum

of pressure fluctuations measured simultaneously in a 20 cm deep bed at a bed elevations of 5.1 cm and 15.2 cm respectively. In the 5.1 cm measurement, both the 3.5 Hz frequency phenomena and the 2.2 Hz frequency behavior can be observed. While the 3.5 Hz frequency spike is not detected in the spectrum of the upper bed, the lower frequency phenomena is evident. This dominant lower frequency that appears at 2.2 Hz will be observed very near 2.2 Hz at all elevations. The Bode plots of fluctuations at all elevations are indicative of second order dynamics. Even above the bed a second order phenomena is observed in the gas fluctuations exiting the bed surface, although it is obvious that fluctuations are significantly damped out at this position (see Figure 3). This observation will be discussed further in connection with turbulent and fast fluidization.

Not only does the elevation at which the pressure fluctuations are measured effect the appearance of the Bode plot profiles, but the spacing of pressure taps can also complicate the observed results. Figures 4 and 5 show the how the tap spacing can distort the observed results. In these figures simultaneous fluctuation measurements were recorded in a BFB at tap spacing of 2.5 cm and 5.1 cm, respectively. These two Bode plots appear fundamentally different. In the case of the 2.5 cm spacing, a very dominant high frequency peak appears at around 5.5 Hz along with a highly damped 3.1 Hz phenomena that can be observed in the Bode plot. The dominant frequency virtually disappears in fluctuations from the 5.1 cm differential measurement, and a broad 2.2 - 3.1 Hz dominant frequency is observed.

A possible explanation for these apparent inconsistencies in the fluctuation spectrum is that the increased distance between the pressure taps introduces what could be considered spatial aliasing to the observed signal. An example using the simulated signals of Figures 6 and 7 best illustrates this concept. Figure 6 shows a possible distribution of local voidages across the height of a fluidized bed. This voidage distribution can be thought of as a series of bubble layers passing up through the fluidized bed. Differential pressure measurements record the average pressure or voidage between the taps. By averaging the local voidage measurements between the two tap configurations in Figure 6 (taps across 0-5% and 0-20% bed height), as the wave propagates upwards through the bed, the resulting voidage signal measured for both cases is shown in Figure 7. It is evident that the dominant frequency of the signal measured by the taps between 0-20% bed height is half of that observed in the taps that are closer. If such spatial aliasing was occurring in

the bubbling bed system shown in Figure 5, the 5.5 Hz phenomena should be observed as a 2.2 Hz phenomena. Close inspection of Figure 5 confirms this. Locating the two pressure taps used in the differential measurement close together will decrease the chances of spatial aliasing effects. Although, if the taps are placed too close to one another the magnitude of the fluctuation will not be large enough to be accurately recorded by most transducers, and noise may begin to mask the system dynamics.

Considering that both the method of pressure fluctuation measurement and the method of pressure fluctuation analysis (as described in previous reports), make a significant difference in the observed results, it is not surprising that there is still no consensus as to the phenomena governing pressure fluctuations.

The Nature of Bubbling Fluidized Bed Pressure Fluctuations

A number of general characteristics of bubbling fluidized bed pressure fluctuations have been observed by previous researchers and in the present study as well. Under conditions of low to moderate velocity bubbling fluidization, the particle size does not have a significant effect on the overall dynamic character of the fluctuations. Figures 8 - 10 show three Bode plots of fluctuations taken from similar beds of 0.2 mm, 0.3 mm, and 0.4 mm glass beads fluidized at U/U_{mf}= 1.4. The profiles for each particle size are identical. Any slight variations in the dominant frequency as the particle diameter is changed, are likely due to variations in bubble properties or bed voidage. For further verification that particle diameter does not strongly influence the frequency of the system see Figures 10-13 and Figure 21.

Bed diameter has a significant effect on the Bode plot profiles, although it is important to emphasize that bed diameter does not effect the position at which dominant system frequencies observed until the bubbling regime approaches slugging or turbulent conditions. Figures 14 and 15 show the Bode plots of the 10.2 and 5.1 cm diameter beds respectively. In both beds the particle size, bed height, tap height & spacing, and superficial velocity are identical. It is evident that changes is the diameter can significantly effect the frequency response, changing the degree of damping of the observed frequency. Despite the increased damping, the natural frequencies at which the bed operates under do not change. In both figures, dominant frequencies appear at 3.1 and 5.5 Hz, although the higher (5.5Hz) frequency dominates as the bed diameter decreases.

As shown in Figures 10 - 13, for $U/U_{mf} > 1.2$, changes in the superficial velocity does not effect the dominant frequency in the bubbling fluidization regime. At the onset of fluidization, the dominant frequency increases only slightly and then levels off as the superficial velocity is increased above $U/U_{mf} > 1.2$. It should again be emphasized that the superficial velocity will not change the characteristic period of oscillation of the system, but it may dictate the damping of the observed frequencies in the spectrum.

BFB Pressure Fluctuations as a Global Phenomena

Our work suggests that two different types of global phenomena are responsible for pressure fluctuations in bubbling fluidized beds. Our research has led us to dismiss the possibility of a random local phenomena (such as bubbles) as being the complete explanation of the origin of pressure fluctuations in bubbling beds for two reasons. Static pressure measurements in a BFB were simultaneously recorded from the center of the bed and at the bed wall. The Bode plot profiles of the fluctuations at these two locations were identical. If the passage of local bubbles was solely responsible for pressure fluctuations, the hydrodynamics at the center of the bed would produce a different fluctuation structure, since the majority of bubbles rise to the surface through the center of the bed. Further evidence of the global nature of pressure fluctuations was obtained from an experiment in which two different drilled hole distributor plates were tested under identical operating conditions. The two distributor plates had the same total hole-area, but one had 72 holes while the other had only 36 holes. Since bubbles form at the distributor plate holes, the 72 hole plate would produce more bubbles than the 36 hole plate. As is shown in Figures 17 - 18, the Bode plots of the pressure fluctuations from the two different distributor plate cases are identical, suggesting that random bubble passage in the vicinity of the region of pressure measurement is not a sufficient explanation for the observed fluctuations. This argument does not lead to the conclusion that bubbles are not responsible for pressure fluctuation phenomena, but rather that the global phenomena that dictates fluidized bed hydrodynamics may also govern the periodic production of bubbles.

Evaluation of the Global Theories of Fluidized Bed Oscillations

Three different categories of global phenomena are highlighted by Roy and Davidson [3]: a natural frequency of oscillation of the entire bed; a surface phenomena that propagates pressure fluctuations down through the bed; and a plenum compression wave phenomena exhibited in fluidized beds with low resistance distributor plates. This third phenomena is not of interest in this study. To eliminate the effect of this phenomena, high resistance distributor plates are used. It is hypothesized that two global fluidization phenomena are responsible for the structure of fluctuations. These two phenomena will be generally referred to as the natural frequency and the surface frequency.

When evaluating potential theories for the origin of fluctuations in bubbling beds, two requirements must be considered. The first requirement is that the theory must be able to account for the second order system behavior observed in fluidized bed systems. The Bode plots of all fluidized bed systems exhibit a final asymptotic slope of -40 dB/decade. Figures 19 and 20 show examples of simple second order systems. In many cases, a single second order system is not sufficient to describe fluidization hydrodynamics. Experiments suggest that the dynamics of fluidization can be described by a model that assumes multiple second order systems acting concurrently within the fluidized bed system. Second order systems acting in parallel will also yield -40 dB/decade final Bode plot roll off (as shown by example in Figure 21). Secondly, the theory must be able to predict the observed dominant frequencies accurately and explain why at low bed heights they appear to be inversely proportional to the square root of bed height.

There are three researchers who have proposed mechanisms that meet these two requirements. The first two researchers to present mechanisms for fluctuations were Hiby [4] and Verloop [5]. Fundamentally the mechanism proposed by both these researchers is the same, although the derivations differ slightly. While Verloop maintains that the entire incipiently fluidized bed oscillates in phase, Hiby proposes a system of oscillating layers being "pulled into tune." The changes in bed voidage as the bed lifts and returns to its initial position result in the fluctuations of static pressure drop across the bed. While Verloop focuses on shallow incipiently fluidized beds, Hiby extends this phenomena to explain layers of bubble production which coincide with the natural oscillations of the bed.

Baskakov [6] takes a different approach to fluidized bed dynamics. He proposes a direct analogy between fluidized bed dynamics and a hydraulic pendulum (e.g. U-tube manometer). For Baskakov the changes in voidage (or pressure) are due to changes in the height of the surface caused by the rise of a large single bubble. As the bubble rises through the bed it entrain solids to the top of the bed, causing the bed surface to rise. The solids return downward along the sides of the bed to restore the bed to its equilibrium condition. This cyclic movement of solids up the center of the bed via bubbles and back down the sides via annular flow constitutes Baskakov's oscillatory pendulum. The primary weakness of Baskakov's theory lies in the validity of the hydraulic pendulum analogy. The simplifying assumptions that go into this analogy are not convincing. Baskakov's derivation is based on the U-tube manometer not a fluidized bed system. He simply assumes a direct analogy can be made to the fluidized bed. Secondly, Baskakov's model is dependent on bubbles as a forcing mechanism; he does not explain the possibility or origin of the necessary periodic bubble formations.

In all three theories, the experimental data that Hiby publishes for incipiently fluidized beds fits relatively well with the predicted frequency, although Hiby's own relation provides the best fit. The relations derived for the natural frequency of the bed proposed by the authors above is summarized below:

Hiby (1967)
$$\omega = \sqrt{\frac{g \cdot (1-\varepsilon)}{(0.75 \cdot \pi^2) \cdot H \cdot \varepsilon}} \tag{1}$$

Verloop (1974)
$$\omega = \frac{1}{2 \cdot \pi} \sqrt{\frac{g \cdot (2-\varepsilon)}{H \cdot \varepsilon}} \tag{2}$$

Baskakov (1986)
$$\omega = \frac{1}{\pi} \sqrt{\frac{g}{H}} \tag{3}$$

The reason for preferring Hiby's relation over Verloop's similar derivation is because it better predicts the observed frequency. The experimental evidence from this study of bubbling bed fluctuations supports Hiby's hypothesis that the natural bed frequency may dictate the bubble production frequency. Figures 22 through 29 show how experimental data gathered from this studies bubbling bed systems compare with the models above (using $\varepsilon = 0.49$). Clearly, Hiby's model comes the closest to predicting the observed dominant frequency even in bubbling fluidized beds. The relations of Hiby and Verloop differ from Baskakov's relation in two significant ways.

First, the assumptions involved in the derivation of Hiby and Verloop's relations are based on fluidized bed hydrodynamics, rather than simply the dynamics of a U-tube pendulum. Secondly, as seen by comparing equations 1 - 3, Baskakov's relation proposes that the fundamental frequency is not a function of the bed voidage, as it is in the Verloop and Hiby relations. While Baskakov asserts that experiments show that the frequency is independent of voidage, no conclusive experimental data has ever been published that definitively supports this claim. Our experimental data was not taken in such a manner to confirm either hypothesis. In order to support such a claim, an accurate means of measuring the overall bed voidage must be used. Also, typically the range of fluidization voidages is very small (e.g. 0.46-0.49) making a systematic study of the effect of voidage difficult. For these reasons, Hiby's relation seems to be the most plausible theory to explain the oscillatory behavior in bubbling fluidized bed systems, but as will be shown in the following section, this theory has a fundamental error in its assumptions. By correcting this assumption, a modified Hiby formulation is derived that better predicts the observed frequency.

Since only Hiby's data for incipient fluidization was used for comparison to these theories, it was not observed that as the bed height increases to heights greater than 10 cm, multiple peaks begin appearing in the spectrum, complicating the overall system (see Figures 23 and 24). As the bed height increases the frequency tends to be at a lower frequency than predicted by theories for natural bed oscillations. Increasing the height increases bubble coalescence, resulting in the upper surface lifting or erupting from its equilibrium position. Throughout the bed, this subsequent oscillation of the surface can be detected concurrently with natural bed oscillations. In very deep beds significant coalescence occurs and the surface fluctuations will occur at a slightly lower frequency than the natural bed frequency. This surface effect will begin to interfere with the natural oscillation of the bed such that the observed frequency is less than the predicted value inversely proportional to the square root of the bed height. This effect produced by excessive bubble coalescence was not observed by other researchers since previous experimental data was recorded in beds that were operated at incipient fluidization conditions only. The decrease in the fluctuation frequency due to this surface phenomena is most pronounced as the particle size decreases. For large particle sizes, the slope observed on the log-log plot of frequency versus bed height is close to the -0.5 predicted by theory (see Figure 28). For smaller particle sizes the slope

becomes steeper and seems to approach a slope closer to -1.0 as the bed height increases (see Figures 26 and 27). Smaller particles will tend to produce smaller bubbles. These smaller bubbles will rise faster, increasing the rate of bubble coalescence. As coalescence increases, the surface eruption frequency decreases due to the fewer (but larger) bubbles at the bed surface. Figure 29 shows how the observed frequencies are complicated in small diameter beds, or more specifically, beds with a high H/D ratio. Again, this is due to bubble coalescence, which will increase as the height is increased, and to slugging behavior which increases as the diameter is reduced.

Derivation of a Modified-Hiby Model for Bubbling Fluidized Bed Dynamics

While Hiby's research provides the most plausible theory and rigorous derivation to date, he makes a fundamental error in the assumptions used in his theoretical derivation. By correcting this error, a more accurate relation can be developed to both predict the natural frequency and explain the second order dynamics observed in the BFB pressure fluctuations. Hiby begins his derivation by considering a single particle suspended in a fluidized bed [4]. If this particle is displaced from its equilibrium position (either upwards or downwards), the forces on the particle are altered in such a way to bring it back to its equilibrium position. The number of particles in a fluidized bed can be defined as:

$$N = \frac{V_s}{V_p} = \frac{V \cdot (1-\varepsilon)}{\left(\frac{\pi}{6}\right) \cdot d_p^{\,3}} \tag{4}$$

The force acting on a single particle is the sum of its weight and the drag force exerted by the gas flow (neglecting buoyancy forces which are typically very small in gas fluidization systems). The average drag force on an individual particle can be estimated by dividing the total lifting force acting on the bed ($\Delta p \cdot A$) by the total number of particles.

$$F = -mg + \frac{\pi \cdot \Delta p \cdot A \cdot d_p^{\,3}}{6 \cdot V \cdot (1-\varepsilon)} \tag{5}$$

Substituting A/V = 1/H:

$$F = -mg + \left(\frac{\pi \cdot d_p^{\,3}}{6 \cdot (1-\varepsilon)}\right) \cdot \left(\frac{\Delta p}{H}\right) \tag{6}$$

Under fluidization conditions the pressure drop can be estimated using the Ergun equation at minimum fluidization velocity (U_{mf}). This is where Hiby makes an error in his derivation. He uses the variable U rather than the constant U_{mf} to estimate the pressure drop in an incipiently fluidized bed. While at incipient conditions these will be equal by definition, his use of U rather than U_{mf} leads him to some faulty conclusions, as will be shown later. From the Ergun equation:

$$\frac{\Delta p}{H} = 150 \cdot \frac{U_{mf} \cdot \mu}{d_p^{\,2}} \cdot \frac{(1-\varepsilon)^2}{\varepsilon^3} + 1.75 \cdot \frac{\rho_g \cdot U_{mf}^{\,2}}{d_p} \cdot \frac{(1-\varepsilon)}{\varepsilon^3} \tag{7}$$

Therefore:

$$F = -mg + \left(\frac{\pi \cdot d_p^{\,3}}{6}\right) \cdot \left(150 \cdot \frac{U_{mf} \cdot \mu}{d_p^{\,2}} \cdot \frac{(1-\varepsilon)}{\varepsilon^3} + 1.75 \cdot \frac{\rho_g \cdot U_{mf}^{\,2}}{d_p} \cdot \frac{1}{\varepsilon^3}\right) \tag{8}$$

The assumption is made that all individual particles oscillate such that at every moment all particles show the same relative vertical displacement from their equilibrium position. The oscillation in voidage is only a function of time, and is independent of the height in the bed. Under most normal fluidization conditions the average voidage measured throughout the bed is relatively constant, making this a valid assumption. The amplitude of an individual particle i is then proportional to its height h_i ($a_i \sim h_i$), and,

$$\frac{dh_i}{h_i} = \frac{dH}{H} \tag{9}$$

relating ε to the bed height,

$$\varepsilon = \frac{V - V_s}{V} = 1 - \frac{V_s}{A \cdot H} \tag{10}$$

solving for H,

$$H = \frac{V_s}{A \cdot (1-\varepsilon)} \tag{11}$$

Using Newton's second law we can calculate the natural frequency of an oscillating particle.

Given that: $a_i(t) = -\omega^2 \cdot h_i(t)$

$$F = m_i a_i = -(m_i \cdot \omega_i^{\,2}) \cdot h_i \tag{12}$$

it follows that,

$$\frac{dF}{dh_i} = -\left(m_i \cdot \omega_i^2\right) \tag{13}$$

Solving for ω_i,

$$\omega_i^2 = -\frac{1}{m} \cdot \frac{dF}{dh_i} = -\frac{6}{\pi \cdot d_p^3 \cdot \rho_s} \cdot \frac{dF}{d\varepsilon} \cdot \frac{d\varepsilon}{dh_i} \tag{14}$$

From equation (9),

$$\frac{dH}{dh_i} = \frac{H}{h_i} \tag{15}$$

Differentiating equation (11),

$$\frac{d\varepsilon}{dH} = \frac{V_s}{A \cdot H^2} \tag{16}$$

From equations (16), (15), and (11),

$$\frac{d\varepsilon}{dh_i} = \frac{d\varepsilon}{dH} \cdot \frac{dH}{dh_i} = \frac{V_s}{A \cdot H \cdot h_i} = \frac{1-\varepsilon}{h_i} \tag{17}$$

Differentiating equation (8),

$$\frac{dF}{d\varepsilon} = -\left(\frac{\pi \cdot d_p^3}{6}\right) \cdot \left(150 \cdot \frac{U_{mf} \cdot \mu}{d_p^2} \cdot \frac{3-2\cdot\varepsilon}{\varepsilon^4} + 1.75 \cdot \frac{\rho_g \cdot U_{mf}^2}{d_p} \cdot \frac{3}{\varepsilon^4}\right) \tag{18}$$

Substituting (17) and (18) into equation (14),

$$\omega_i^2 = \frac{3}{\rho_s \cdot h_i} \cdot \left(150 \cdot \frac{U_{mf} \cdot \mu}{d_p^2} \cdot \frac{(1-\varepsilon)\cdot(3-2\cdot\varepsilon)}{3\cdot\varepsilon^4} + 1.75 \cdot \frac{\rho_g \cdot U_{mf}^2}{d_p} \cdot \frac{1-\varepsilon}{\varepsilon^4}\right) \tag{19}$$

Therefore:

$$\omega_i = C_1 \cdot h_i^{-0.5} \tag{20}$$

where

$$C_1 = \sqrt{\frac{3}{\rho_s}\left(150 \cdot \frac{U_{mf} \cdot \mu}{d_p^2} \cdot \frac{(1-\varepsilon)\cdot(3-2\cdot\varepsilon)}{3\cdot\varepsilon^4} + 1.75 \cdot \frac{\rho_g \cdot U_{mf}^2}{d_p} \cdot \frac{1-\varepsilon}{\varepsilon^4}\right)} \tag{21}$$

This shows that the natural frequency of a particle depends on its height in the bed. It is obvious that the bed will tend to oscillate at an overall mean frequency as the bed is "pulled into tune". Hiby estimates this mean frequency by summing up a weighted average based on the amplitude of oscillation of each layer of particles.

$$\omega_m = \frac{\int_0^H C_1 \cdot h^{-0.5} dh}{\int_0^H h dh} = \frac{4}{3} \cdot C_1 \cdot H^{-0.5} \tag{22}$$

therefore,

$$\omega_m = \frac{4}{3}\sqrt{\frac{3}{\rho_s \cdot H} \cdot \left(150 \cdot \frac{U_{mf} \cdot \mu}{d_p^2} \cdot \frac{(1-\varepsilon)\cdot(3-2\cdot\varepsilon)}{3\cdot\varepsilon^4} + 1.75 \cdot \frac{\rho_g \cdot U_{mf}^2}{d_p} \cdot \frac{1-\varepsilon}{\varepsilon^4}\right)} \tag{23}$$

and converting to cycles per second (Hz),

$$\nu_m = \frac{2}{3\cdot\pi}\sqrt{\frac{3}{\rho_s \cdot H} \cdot \left(150 \cdot \frac{U_{mf} \cdot \mu}{d_p^2} \cdot \frac{(1-\varepsilon)\cdot(3-2\cdot\varepsilon)}{3\cdot\varepsilon^4} + 1.75 \cdot \frac{\rho_g \cdot U_{mf}^2}{d_p} \cdot \frac{1-\varepsilon}{\varepsilon^4}\right)} \tag{24}$$

Hiby develops an equation identical to equation 24 except that ν_m is a function of U rather than U_{mf}. Using some algebraic manipulation, and an approximation he arrives at a simplified equation of the form shown in equation 28 below. By initially using the better assumption of U_{mf} rather than U in equation 7 the following relations can be used to simplify the equation 24. For Rep < 20 the first term within the bracket dominates and U_{mf} can be estimated,

$$U_{mf} = \frac{d_p^2 \cdot \rho_s \cdot g}{150 \cdot \mu} \frac{\varepsilon_{mf}^3}{1-\varepsilon_{mf}} \tag{25}$$

Assuming $\varepsilon_{mf} \approx \varepsilon$, the natural frequency from (24) would reduce to:

$$\nu_m = \frac{2}{3\cdot\pi}\sqrt{\frac{g}{H} \cdot \left(\frac{(3-2\cdot\varepsilon)}{\varepsilon}\right)} \tag{26}$$

For Rep > 20 the second term within the bracket dominates and U_{mf} can be estimated,

$$U_{mf} = \sqrt{\frac{d_p \cdot \rho_s \cdot g \cdot \varepsilon_{mf}^3}{1.75 \cdot \rho_g}} \tag{27}$$

Again, assuming $\varepsilon_{mf} \approx \varepsilon$, the natural frequency from (24) would reduce to:

$$\nu_m = \frac{2}{3\cdot\pi}\sqrt{\frac{3\cdot g}{H} \cdot \left(\frac{1-\varepsilon}{\varepsilon}\right)} \tag{28}$$

For this study Re_p is significantly less than twenty and Equation (26) should predict the frequency of oscillation for shallow fluidized beds. Figures 30 and 31 demonstrate that equation 26 more accurately predicts the observed natural frequency than any previously proposed model. The error in Hiby's derivation is made evident as he tries to address his relations dependence on U and

d_p [4]. According to his theory, the superficial velocity and the particle diameter would have a significant effect on the observed frequency. Using his relation, for laminar conditions of flow, $\nu_m \sim U^{-0.31}$ and $\nu_m \sim d_p^{-1}$. For turbulent conditions $\nu_m \sim U^{-1}$ and $\nu_m \sim d_p^{-0.5}$. These predictions are contrary to experimental observations which show frequency to be independent of U and d_p.

In addition to establishing that the modified Hiby relation better predicts the observed natural frequency of the bed, it is evident from the derivation of this dynamic model that pressure fluctuations will exhibit second order behavior. From Newton's second law on a single particle with u(t) as the white noise forcing function and neglecting damping mechanisms:

$$\frac{dh^2_i(t)}{dt^2} + \omega^2 h_i(t) = u(t) \tag{29}$$

Knowing that the change in position is proportional to the change in voidage, and the change in voidage proportional to the change in pressure drop.

$$\frac{d\Delta p^2(t)}{dt^2} + \omega^2 \Delta p(t) = u(t) \tag{30}$$

The modified Hiby relation satisfies the two important criteria for a global dynamic model of shallow fluidized bed systems. It not only predicts well the dominant frequency, but also provides an explanation for the second order pressure fluctuation response observed. The first peak observed in the frequency spectrum is the result of this natural bed frequency.

The second dominant peak that appears in the spectrum of deep beds represents the interference of the surface eruption frequency with the natural bed frequency. Due to the increased coalescence of bubbles, the surface dynamics become more pronounced and nearly equal in magnitude to the natural bed fluctuations. This surface phenomena will have two effects. First, as seen in Figures 1 and 2, this frequency of surface eruption is propagated down throughout the bed and can be observed simultaneously interfering with the pressure fluctuations of the lower bed region. The higher frequency spikes in the spectrum are the result of simultaneously measuring the natural and surface fluctuations which are not acting in phase. Secondly, as this surface phenomena becomes more pronounced, and as bubble coalescence produces surface eruptions at a frequency lower than the natural frequency, this effect begins to pull the natural frequency "out of tune with the bed height" to a lower frequency. This is why the experimental results begin to deviate from the proposed model in Figures 30 and 31 at heights of

around 10 cm. The observed frequency continues to deviate to a greater extent from its predicted value as the bed height and corresponding coalescence continues to increase. In the case of very tall and narrow beds, a third, even higher, frequency peak can be observed in the spectrum. This high frequency is always observed at twice the frequency of the natural bed frequency. It is possible that this is a harmonic overtone of this fundamental natural frequency.

Conclusions and Future Work

The method of measurement of pressure fluctuations can make a significant difference on the observed structure. By positioning the differential pressure taps close together the undesirable effects of spatial aliasing can be avoided. Bubbling bed pressure fluctuations represent the combination second order phenomena acting in parallel. The two phenomena that are observed throughout the bed can be categorized as a natural oscillation phenomena and an oscillatory surface phenomena. The various characteristics observed in BFB fluctuations suggest that:

- For shallow beds and beds operated at or near incipient fluidization, the natural bed frequency dominates the pressure fluctuations, dictating the bubble production frequency (in layers).
- As the bed gets deeper, a slightly lower surface frequency phenomena begins to interfere with the natural frequency, tuning this natural bed oscillation to a lower frequency.
- The higher frequency second peak is the result of simultaneously measuring the increased magnitude surface oscillations and the natural bed frequency, which do not act in phase.
- The third peak is a harmonic of the dominant (natural) bed frequency.

Understanding the physical mechanisms that are responsible for pressure fluctuations and how they are typically manifest in the frequency spectrum, it is possible to use the analysis of pressure fluctuations as a tool to verify that hydrodynamic similitude has been achieved.

Future work will reassess the use of bubbling bed pressure fluctuations as a means to validate BFB similitude relations. By analyzing the fluctuations in the transition regimes between bubbling and circulating fluidization (slugging/turbulent beds), phenomena observed in bubbling beds may also be hypothesized to act in fast fluidization as well. A final assessment of pressure fluctuation data recorded from the industrial scale CFB combustion unit will be presented along with the extended results of a CFB similitude study in cold-flow models.

Works Cited

[1] Davidson, J. F. "The two-phase theory of fluidization: successes and opportunities." *AIChE Symposium Series* 1991, 87(281), 1-12.

[2] Brue, E. "Process model identification of circulating fluidized bed hydrodynamics." M.S. Thesis, Iowa State University, 1994.

[3] Roy, R., J.F. Davidson, and V.G. Tuponogov. "The velocity of sound in fluidized beds." *Chem. Eng. Sci.* 1990, 45(11), 3233-3245.

[4] Hiby, J.W. "Periodic phenomena connected with gas-solid fluidization." In *Proceedings of the International Symposium on Fluidization, Eindhoven*; Netherlands University Press: Amsterdam, 1967; 99.

[5] Verloop, J. and P.M. Heertjes. "Periodic pressure fluctuations in fluidized beds." *Chem. Eng. Science* 1974, 29, 1035-1042.

[6] Baskakov, A.P., V.G. Tuponogov, and N.F. Filippovsky. "A study of pressure fluctuations in a bubbling fluidised bed." *Powder Technology* 1986, 45, 113-117.

Experimental operating conditions			
Bed diameter	10.16 ± 0.01 cm	Bed height	20.0 ± 0.2 cm
Particle diameter	0.30 ± 0.01 mm	Pressure measurement	differential
Particle density	2600 ± 100 kg/m^3	Pressure tap position	Lower - 2.5 cm/Upper - 7.6 cm
Gas density (air)	1.20 ± 0.04 kg/m^3	Avg. voidage bwt. taps	0.48 ± 0.06
Superficial velocity	12.7 ± 0.6 cm/s ($U/U_{mf} = 1.4$)	Experiment number	6-21-1995-14.1

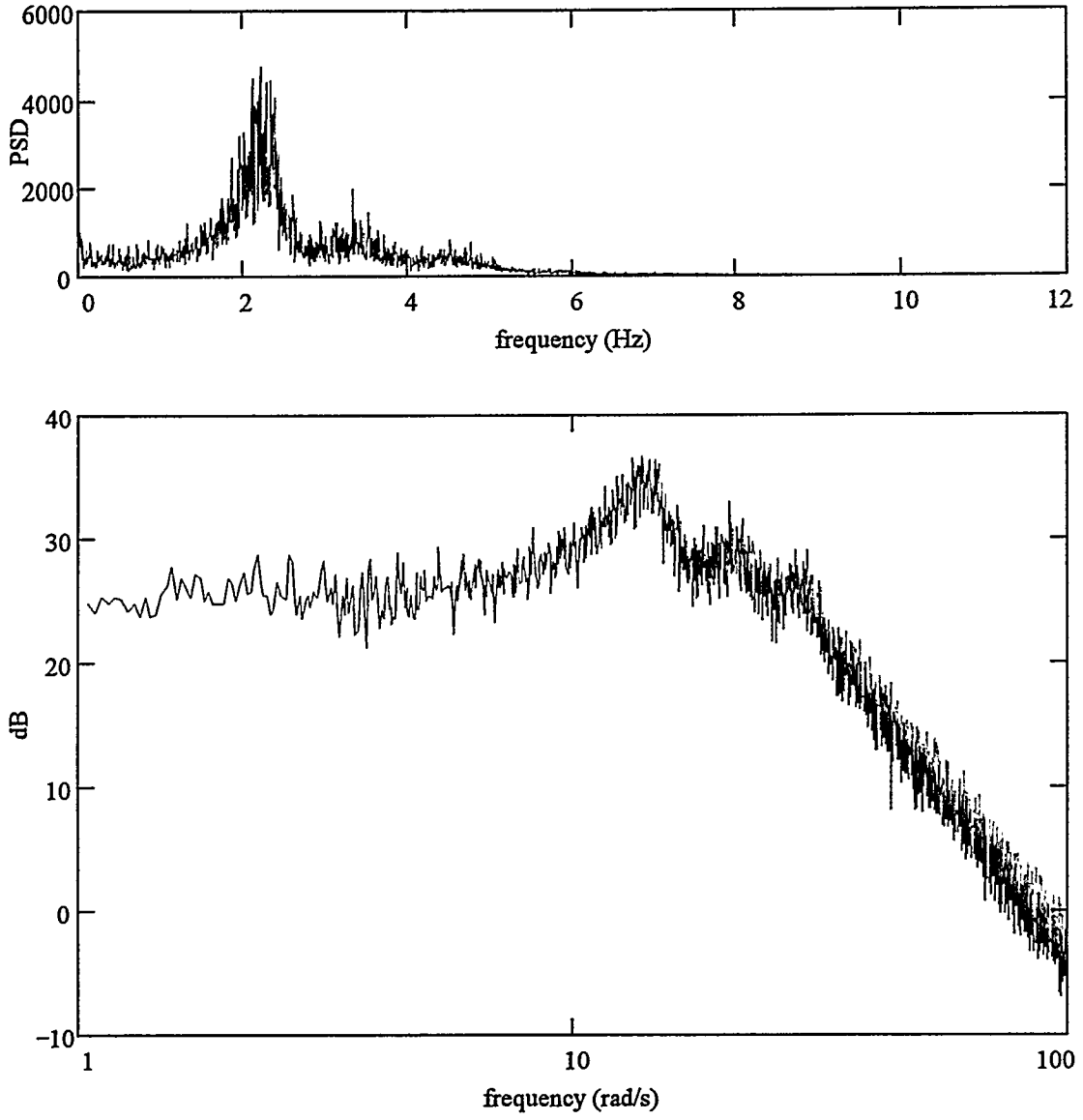

Figure 1: PSD and Bode plot of BFB fluctuations in the lower bed region

Experimental operating conditions			
Bed diameter	10.16 ± 0.01 cm	Bed height	20.0 ± 0.2 cm
Particle diameter	0.30 ± 0.01 mm	Pressure measurement	differential
Particle density	2600 ± 100 kg/m^3	Pressure tap position	Lower-12.7 cm/Upper-17.8 cm
Gas density (air)	1.20 ± 0.04 kg/m^3	Avg. voidage bwt. taps	0.47 ± 0.06
Superficial velocity	12.7 ± 0.6 cm/s ($U/U_{mf} = 1.4$)	Experiment number	6-21-1995-14.1

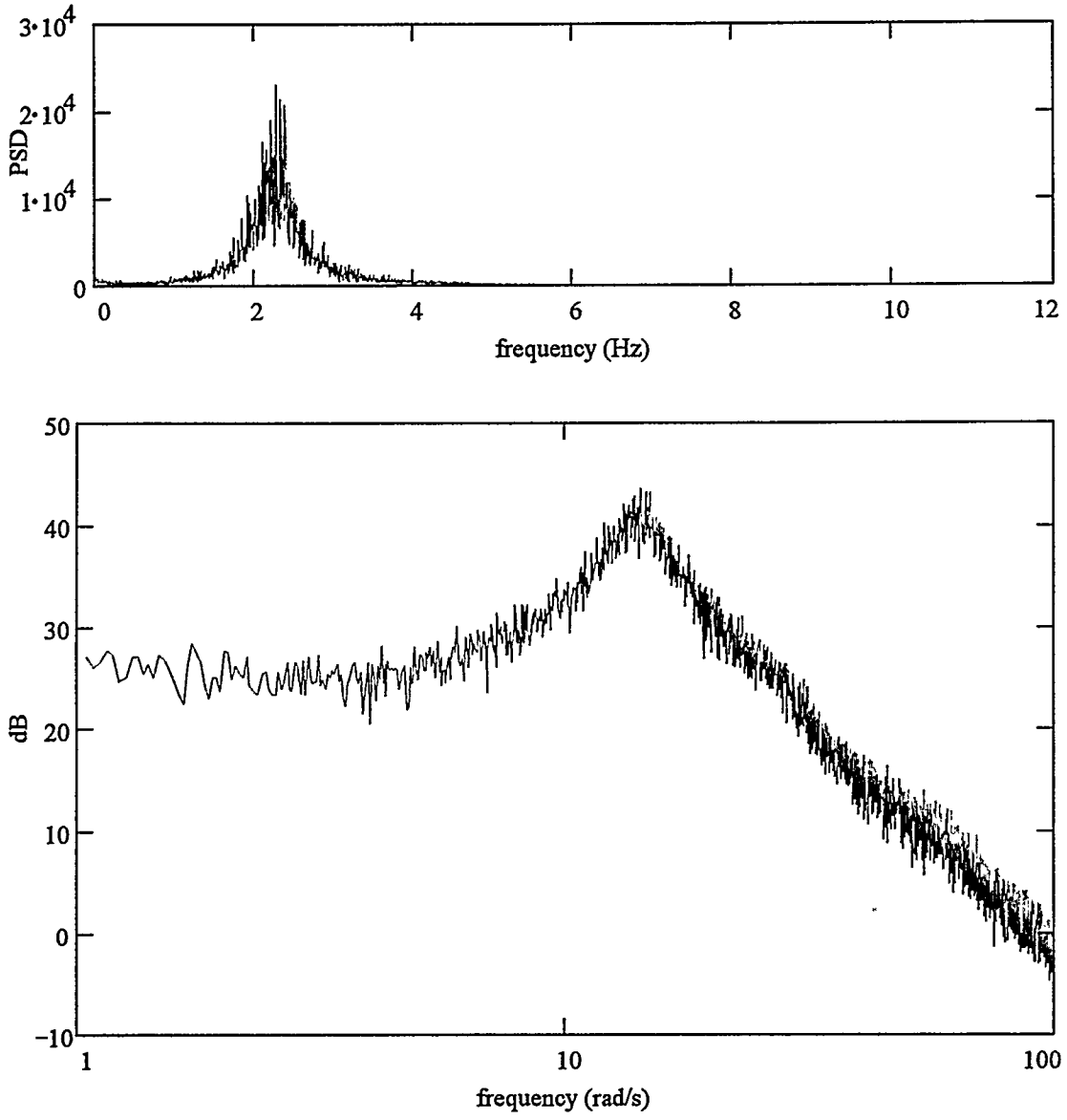

Figure 2: PSD and Bode plot of BFB fluctuations in the upper bed region

Experimental operating conditions			
Bed diameter	10.16 ± 0.01 cm	Bed height	20.0 ± 0.2 cm
Particle diameter	0.30 ± 0.01 mm	Pressure measurement	differential
Particle density	2600 ± 100 kg/m^3	Pressure tap position	Lower-22.9 cm/Upper-27.9 cm
Gas density (air)	1.20 ± 0.04 kg/m^3	Avg. voidage bwt. taps	No particles bwt. taps
Superficial velocity	12.7 ± 0.6 cm/s ($U/U_{mf} = 1.4$)	Experiment number	6-21-1995-14.1

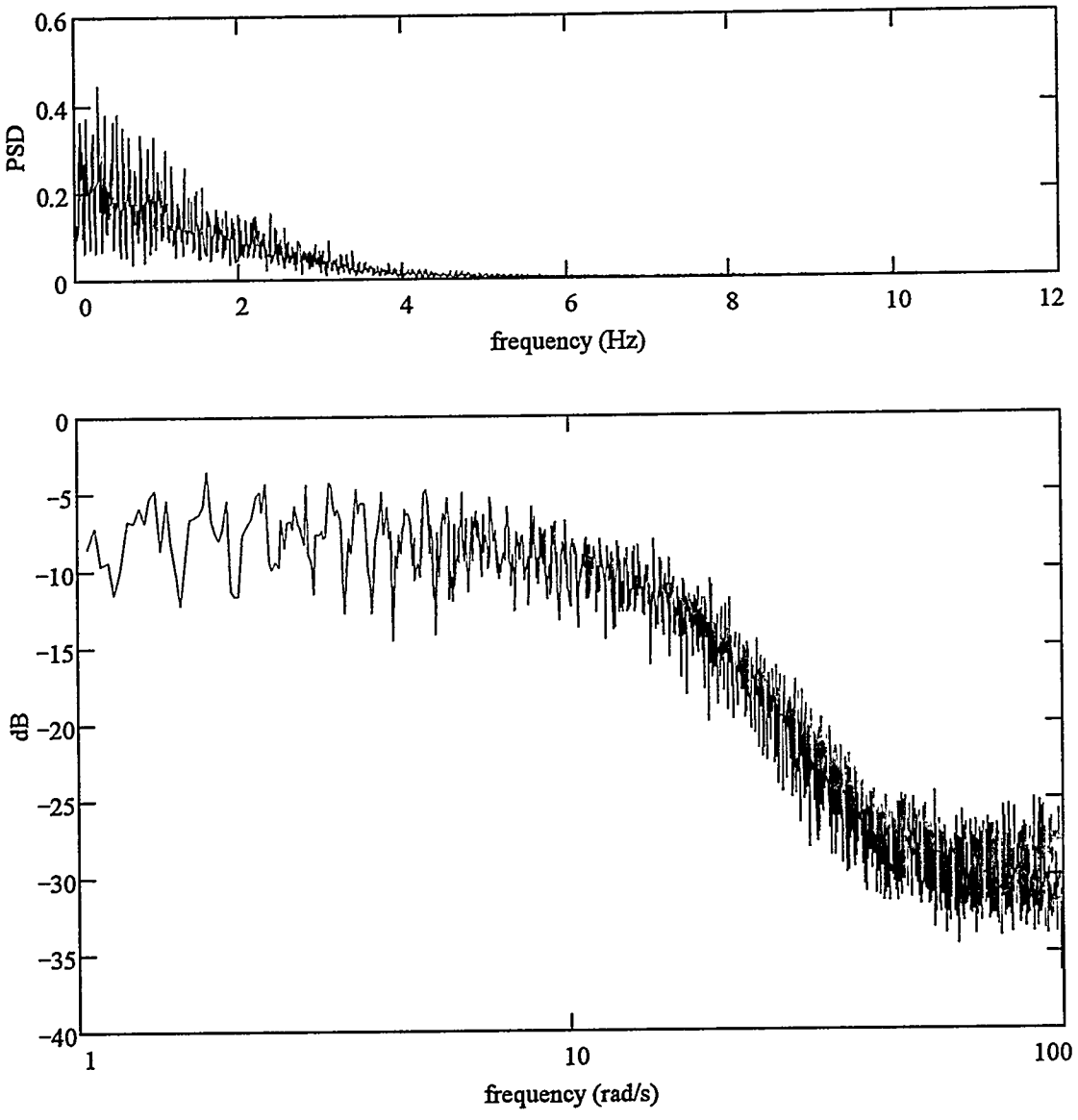

Figure 3: PSD and Bode plot of BFB fluctuations above the bed

Experimental operating conditions			
Bed diameter	5.08 ± 0.01 cm	Bed height	12.0 ± 0.2 cm
Particle diameter	0.20 ± 0.01 mm	Pressure measurement	differential
Particle density	2600 ± 100 kg/m^3	Pressure tap position	Lower - 3.8 cm/Upper - 6.4 cm
Gas density (air)	1.20 ± 0.04 kg/m^3	Avg. voidage bwt. taps	0.48 ± 0.06
Superficial velocity	5.6 ± 0.6 cm/s ($U/U_{mf} = 1.4$)	Experiment number	11-21-1995-11.8

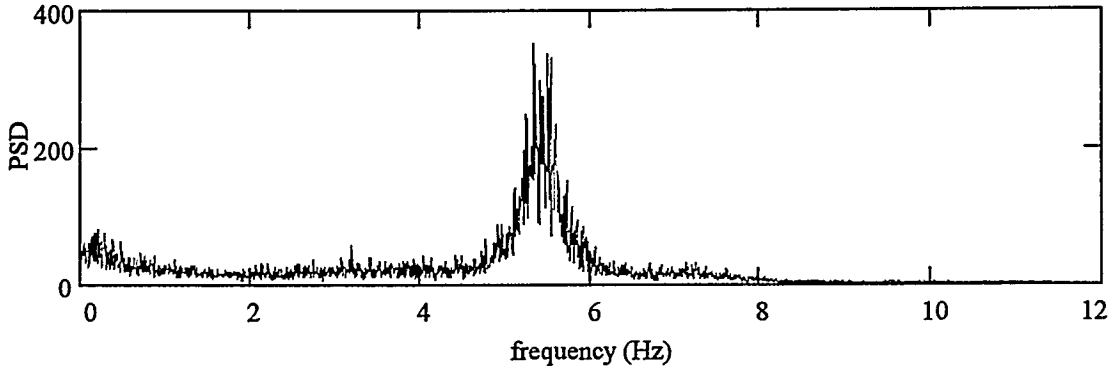

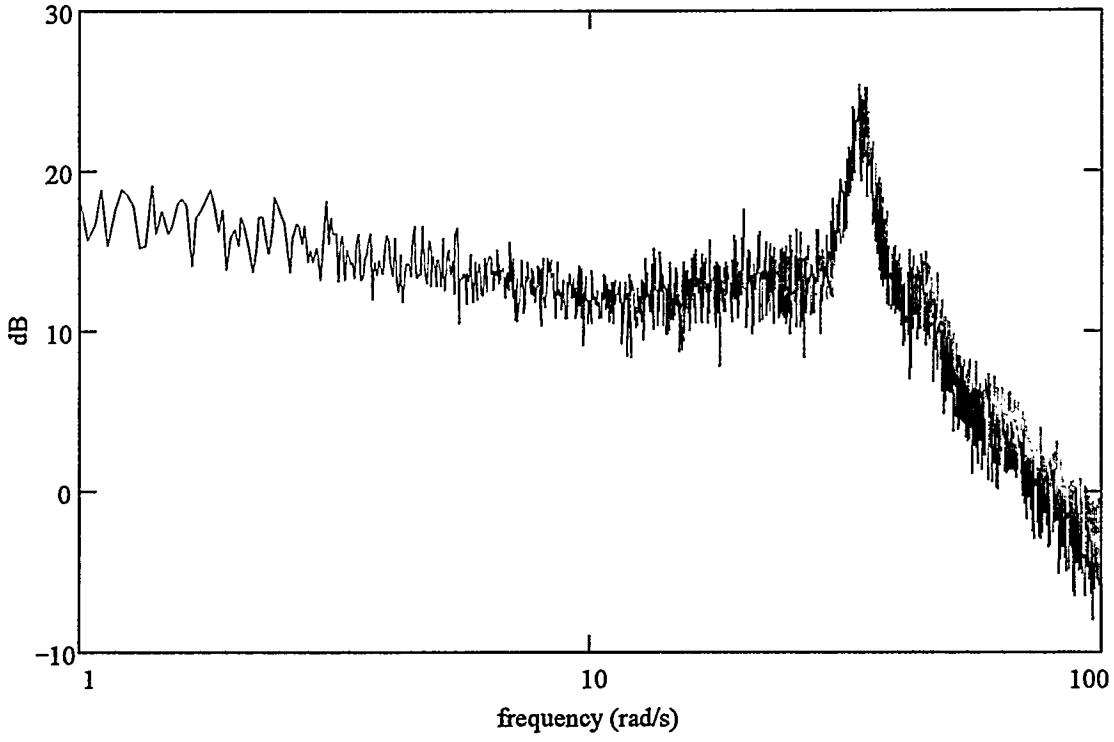

Figure 4: PSD and Bode plot BFB fluctuations with 1.0"(2.5 cm) tap spacing

Experimental operating conditions			
Bed diameter	5.08 ± 0.01 cm	Bed height	12.0 ± 0.2 cm
Particle diameter	0.20 ± 0.01 mm	Pressure measurement	differential
Particle density	2600 ± 100 kg/m^3	Pressure tap position	Lower - 3.8 cm/Upper - 8.9 cm
Gas density (air)	1.20 ± 0.04 kg/m^3	Avg. voidage bwt. taps	0.46 ± 0.09
Superficial velocity	5.6 ± 0.6 cm/s ($U/U_{mf} = 1.4$)	Experiment number	11-21-1995-11.8

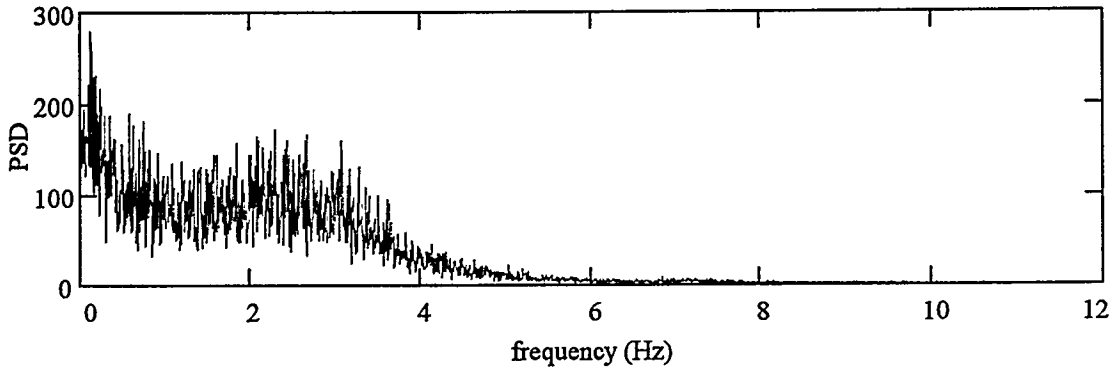

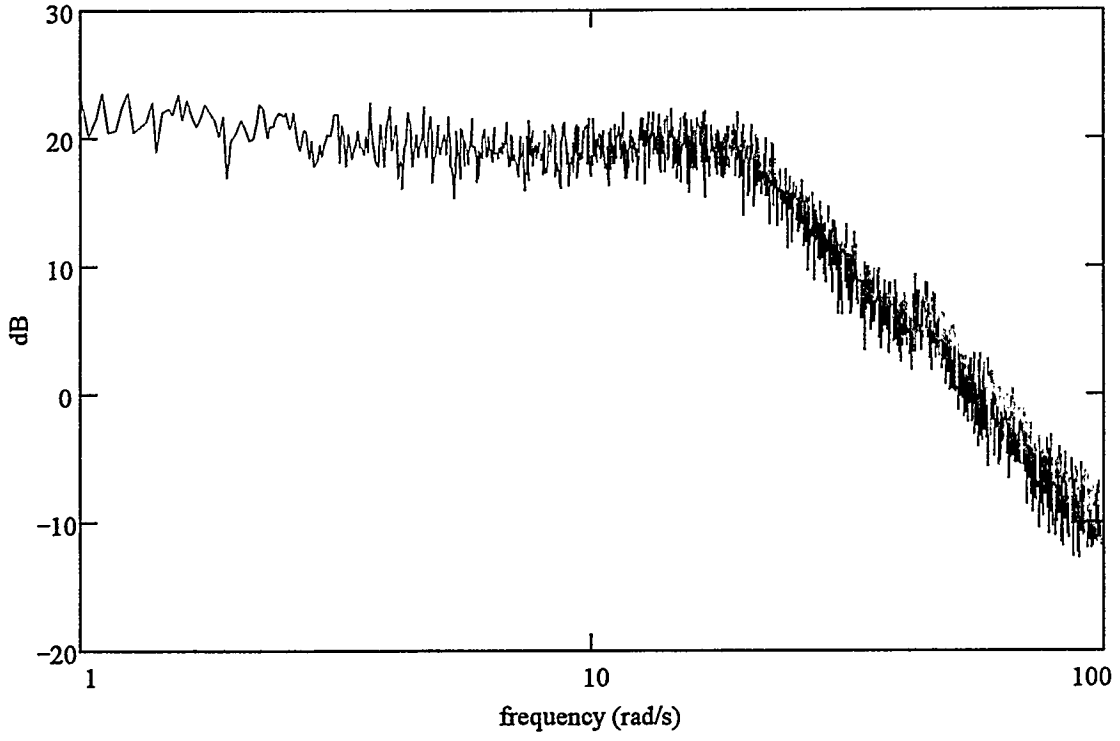

Figure 5: PSD and Bode plot BFB fluctuations with 2.0"(5.1 cm) tap spacing

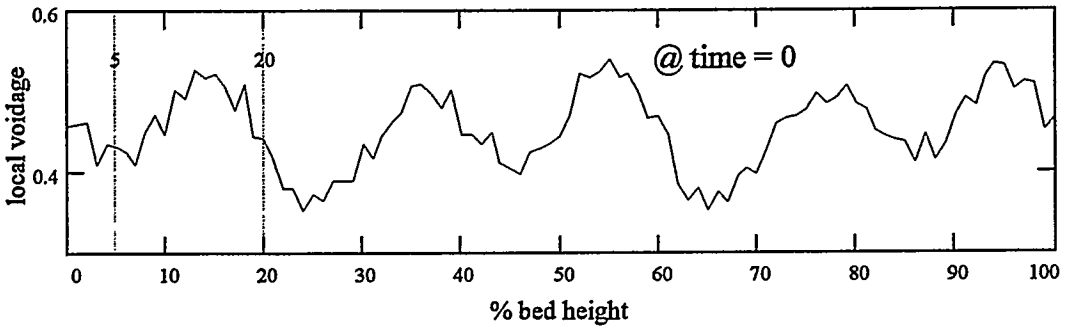

Figure 6: Example of voidage variations across fluidized bed at given time

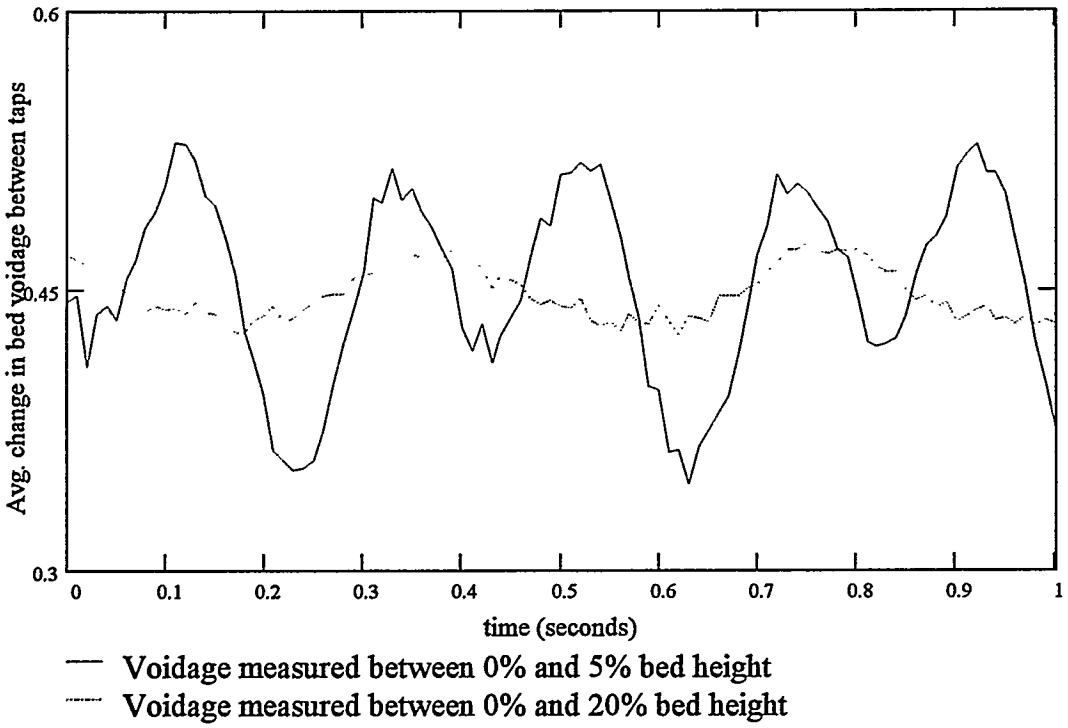

Figure 7: Example - measured average voidage at two different tap spacings

Experimental operating conditions			
Bed diameter	10.16 ± 0.01 cm	Bed height	10.0 ± 0.2 cm
Particle diameter	0.20 ± 0.01 mm	Pressure measurement	differential
Particle density	2600 ± 100 kg/m^3	Pressure tap position	Lower - 2.5 cm/Upper - 7.6 cm
Gas density (air)	1.20 ± 0.04 kg/m^3	Avg. voidage bwt. taps	0.49 ± 0.06
Superficial velocity	5.7 ± 0.6 cm/s ($U/U_{mf} = 1.4$)	Experiment number	6-30-1995-11.1

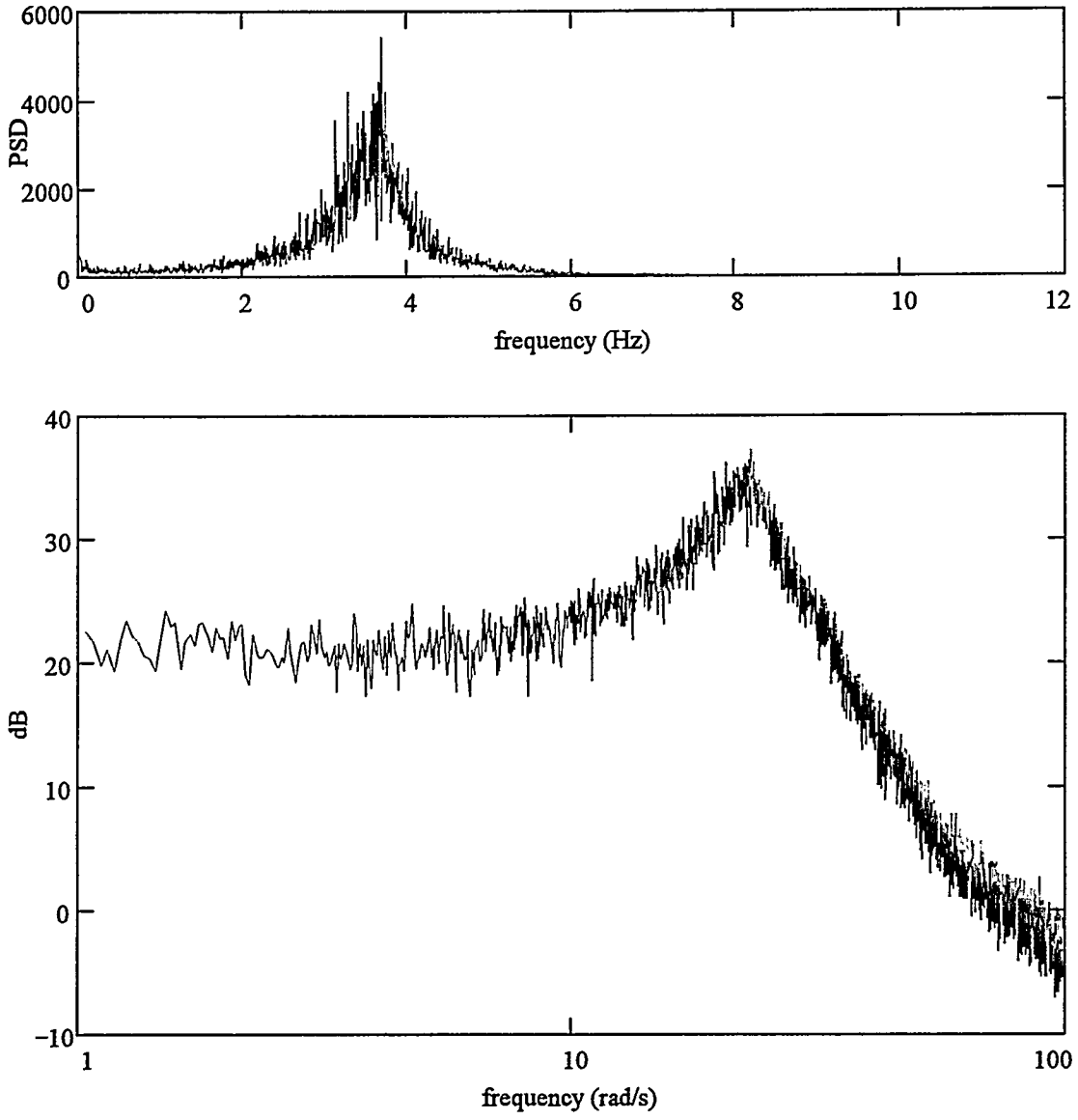

Figure 8 PSD and Bode plot of 0.2 mm glass bead BFB fluctuations

Experimental operating conditions			
Bed diameter	10.16 ± 0.01 cm	Bed height	10.0 ± 0.2 cm
Particle diameter	0.30 ± 0.01 mm	Pressure measurement	differential
Particle density	2600 ± 100 kg/m^3	Pressure tap position	Lower - 2.5 cm/Upper - 7.6 cm
Gas density (air)	1.20 ± 0.04 kg/m^3	Avg. voidage bwt. taps	0.49 ± 0.06
Superficial velocity	12.7 ± 0.6 cm/s ($U/U_{mf} = 1.4$)	Experiment number	6-22-1995-16.4

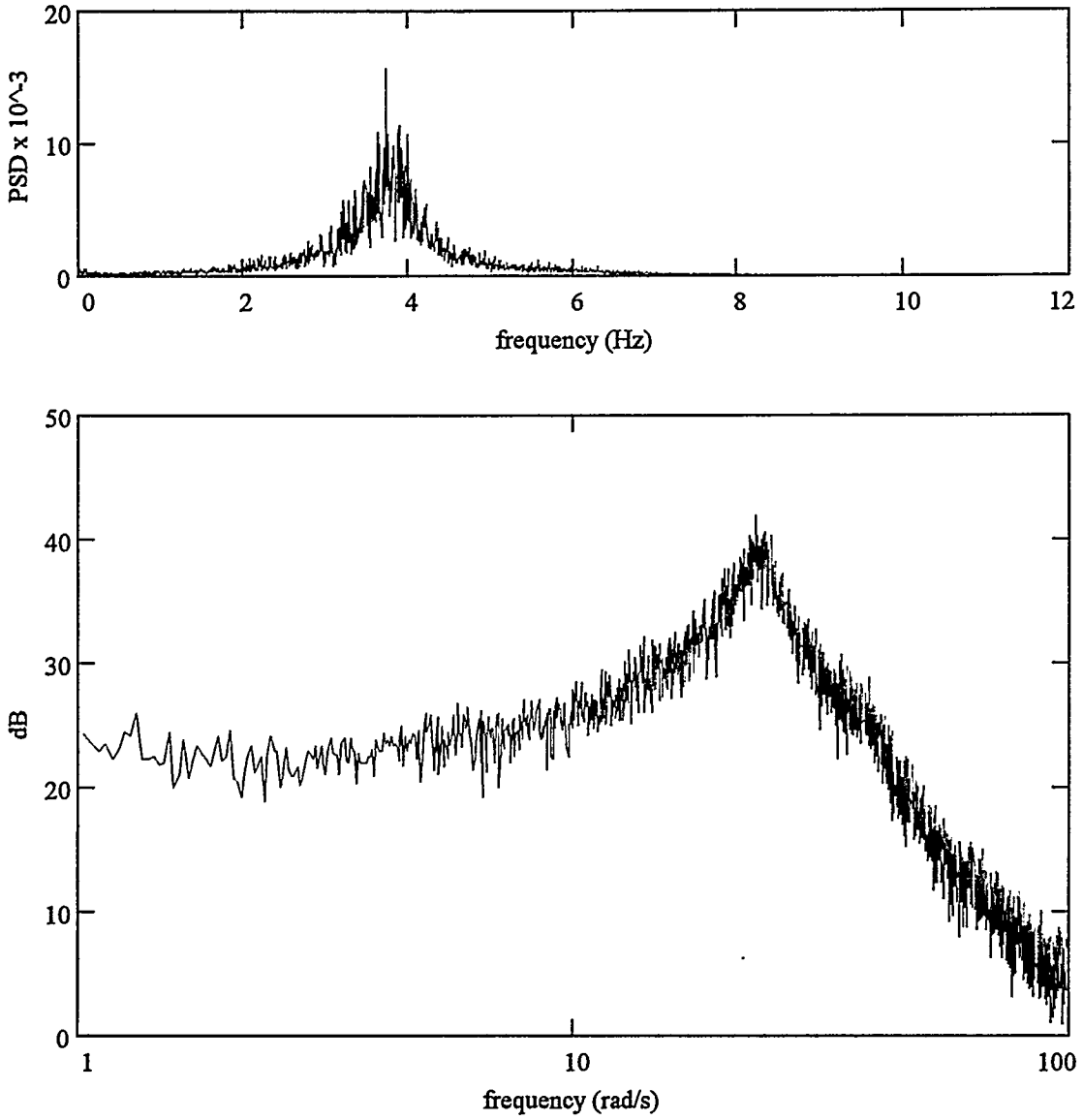

Figure 9: PSD and Bode plot of 0.3 mm glass bead BFB fluctuations

Experimental operating conditions			
Bed diameter	10.16 ± 0.01 cm	Bed height	10.0 ± 0.2 cm
Particle diameter	0.40 ± 0.01 mm	Pressure measurement	differential
Particle density	2600 ± 100 kg/m^3	Pressure tap position	Lower - 2.5 cm/Upper - 7.6 cm
Gas density (air)	1.20 ± 0.04 kg/m^3	Avg. voidage bwt. taps	0.50 ± 0.06
Superficial velocity	19.6 ± 0.6 cm/s ($U/U_{mf} = 1.4$)	Experiment number	7-3-1995-8.4

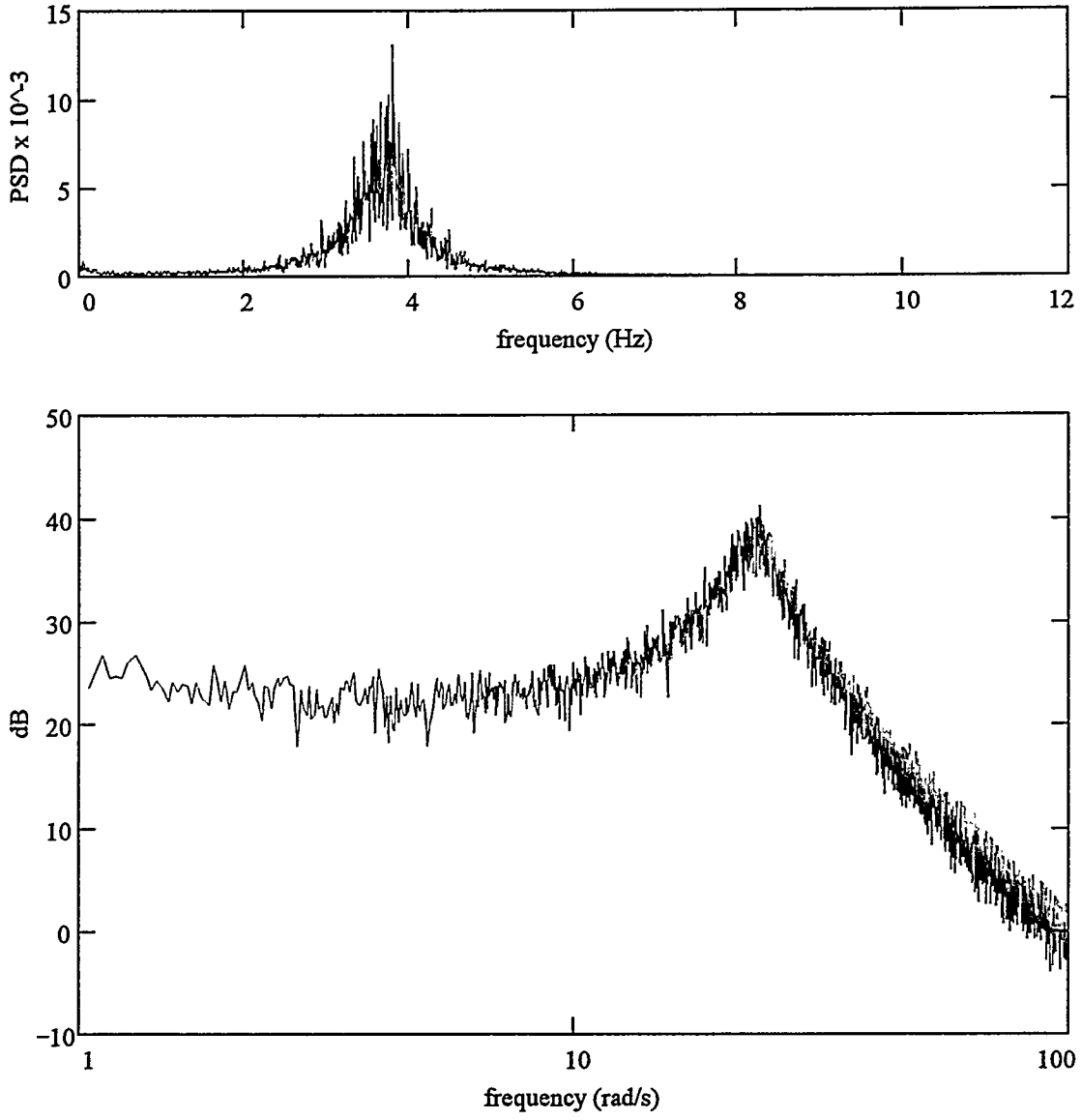

Figure 10: PSD and Bode plot of 0.4 mm glass bead BFB fluctuation

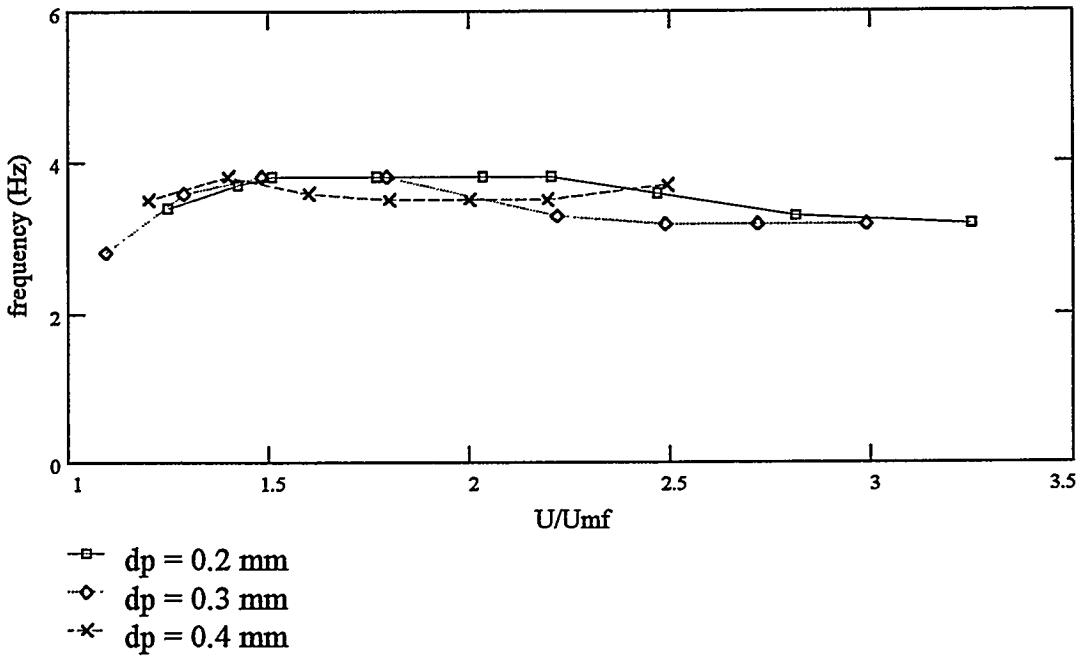

Figure 11: Fluctuation frequency versus U/Umf for 10.0 cm bed height

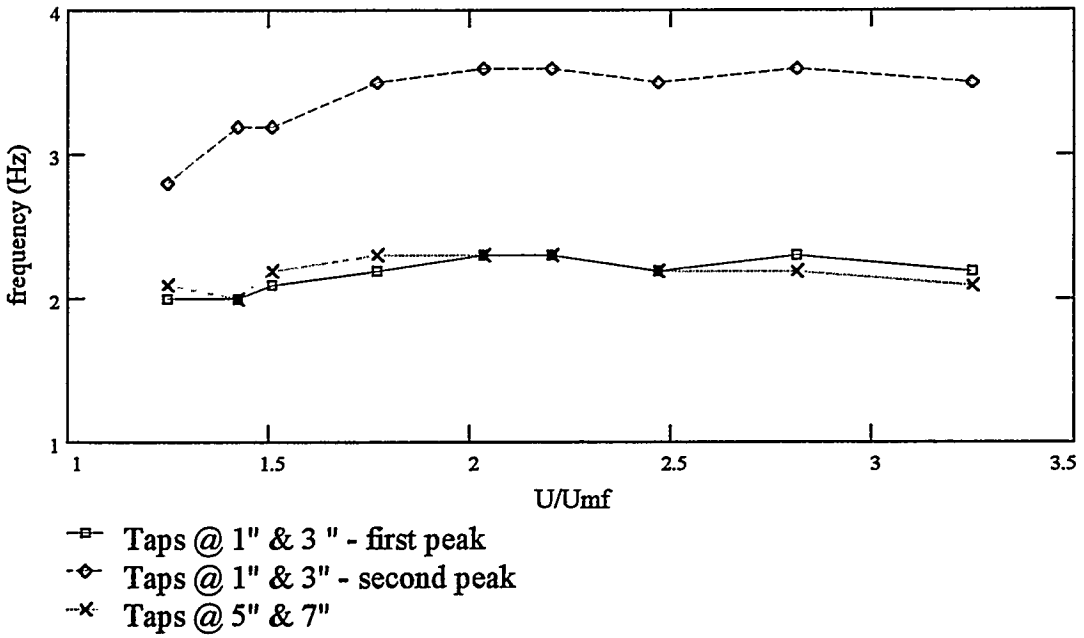

Figure 12: Fluctuation frequency versus U/Umf for 20 cm bed height and dp = 0.2 mm

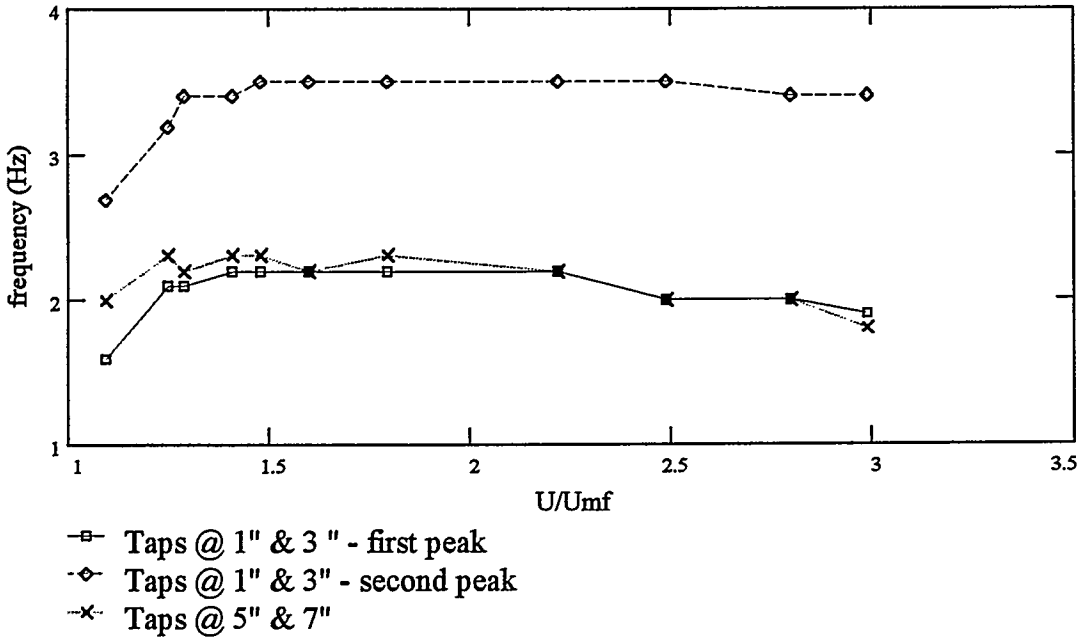

Figure 13: Fluctuation frequency versus U/Umf for 20 cm bed height and dp = 0.3 mm

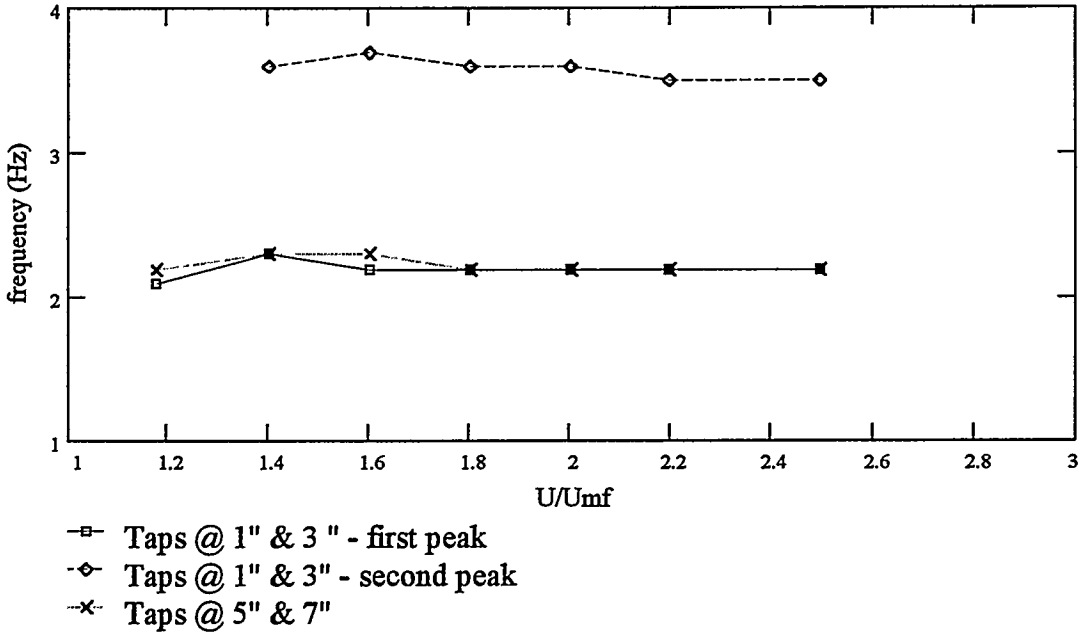

Figure 14: Fluctuation frequency versus U/Umf for 20 cm bed height and dp = 0.4 mm

Experimental operating conditions			
Bed diameter	5.08 ± 0.01 cm	Bed height	12.0 ± 0.2 cm
Particle diameter	0.20 ± 0.01 mm	Pressure measurement	differential
Particle density	2600 ± 100 kg/m^3	Pressure tap position	Lower - 3.8 cm/Upper - 6.4 cm
Gas density (air)	1.20 ± 0.04 kg/m^3	Avg. voidage bwt. taps	0.48 ± 0.06
Superficial velocity	5.6 ± 0.6 cm/s (U/U_{mf} = 1.4)	Experiment number	11-21-1995-11.8

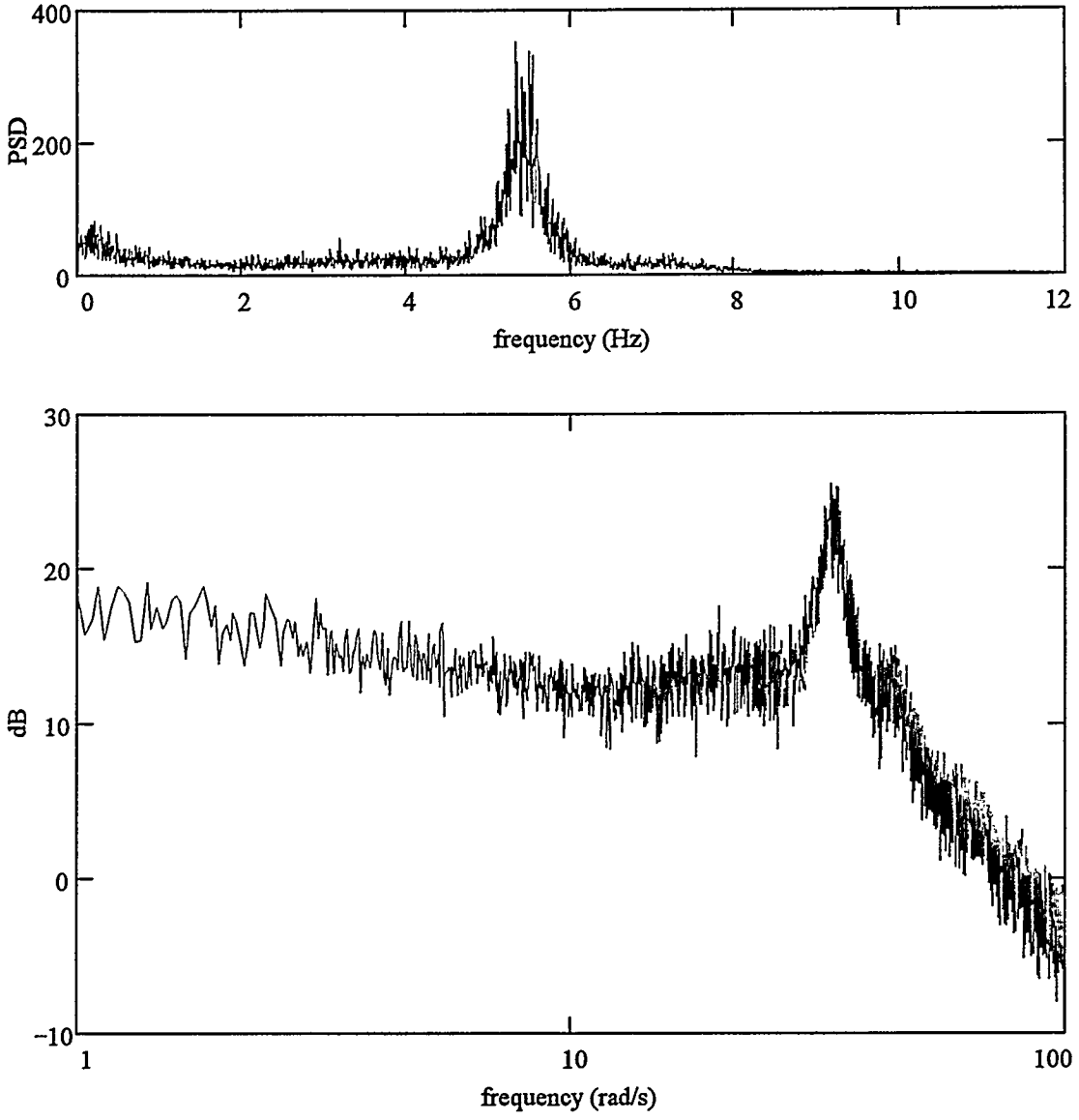

Figure 15: PSD and Bode plot of BFB fluctuations in 5.1 cm diameter bed

Experimental operating conditions			
Bed diameter	10.16 ± 0.01 cm	Bed height	12.0 ± 0.2 cm
Particle diameter	0.20 ± 0.01 mm	Pressure measurement	differential
Particle density	2600 ± 100 kg/m^3	Pressure tap position	Lower - 3.8 cm/Upper - 6.4 cm
Gas density (air)	1.20 ± 0.04 kg/m^3	Avg. voidage bwt. taps	0.48 ± 0.06
Superficial velocity	5.6 ± 0.6 cm/s (U/U_{mf} = 1.4)	Experiment number	11-21-1995-11.8

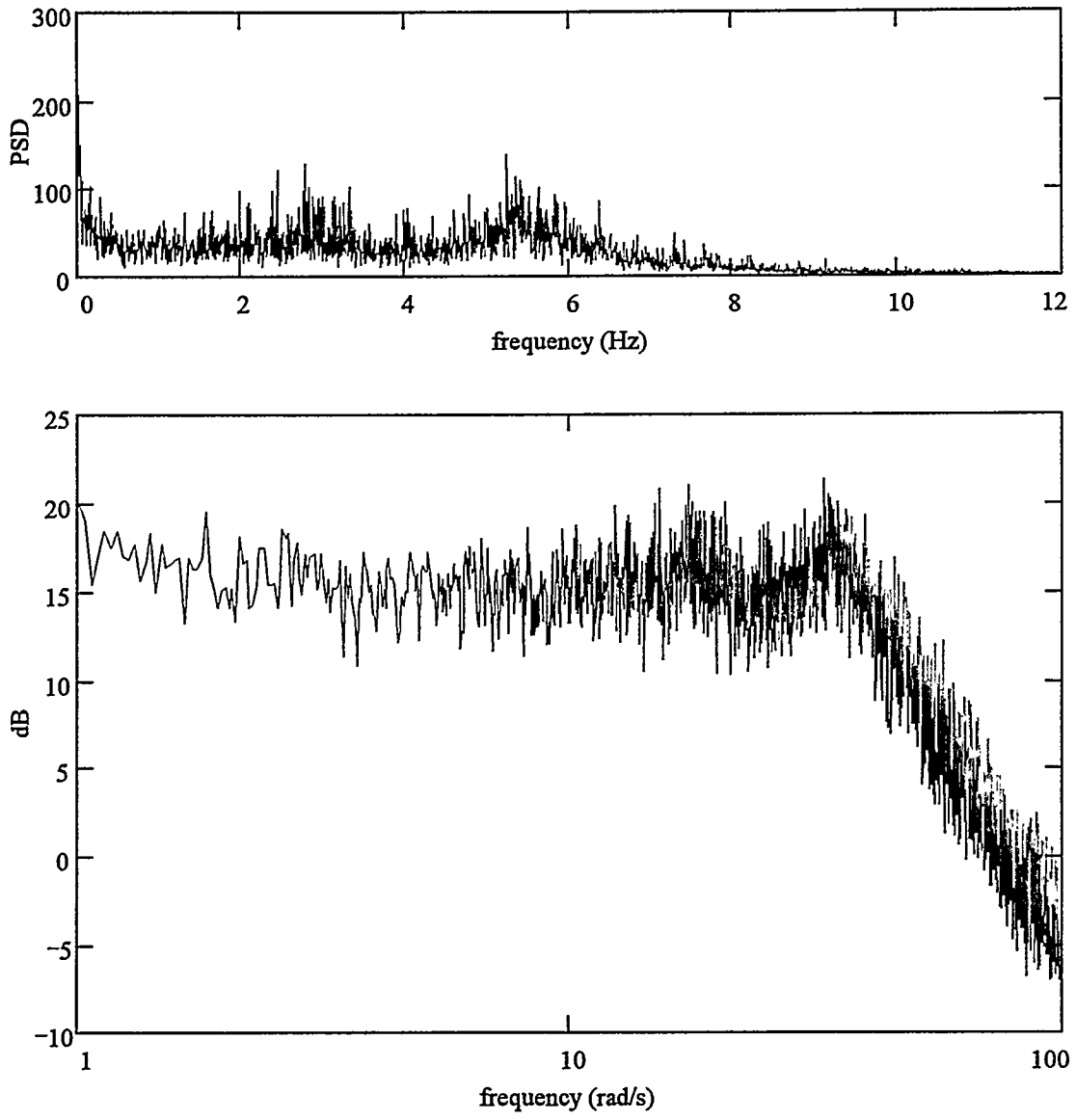

Figure 16: PSD and Bode plot of BFB fluctuations in 10.2 cm diameter bed

Experimental operating conditions			
Bed diameter	10.16 ± 0.01 cm	Bed height	10.0 ± 0.2 cm
Particle diameter	0.40 ± 0.01 mm	Pressure measurement	differential
Particle density	2600 ± 100 kg/m^3	Pressure tap position	Lower - 2.5 cm/Upper - 7.6 cm
Gas density (air)	1.20 ± 0.04 kg/m^3	Avg. voidage bwt. taps	0.50 ± 0.06
Superficial velocity	19.6 ± 0.6 cm/s ($U/U_{mf} = 1.4$)	Experiment number	7-7-1995-11.6

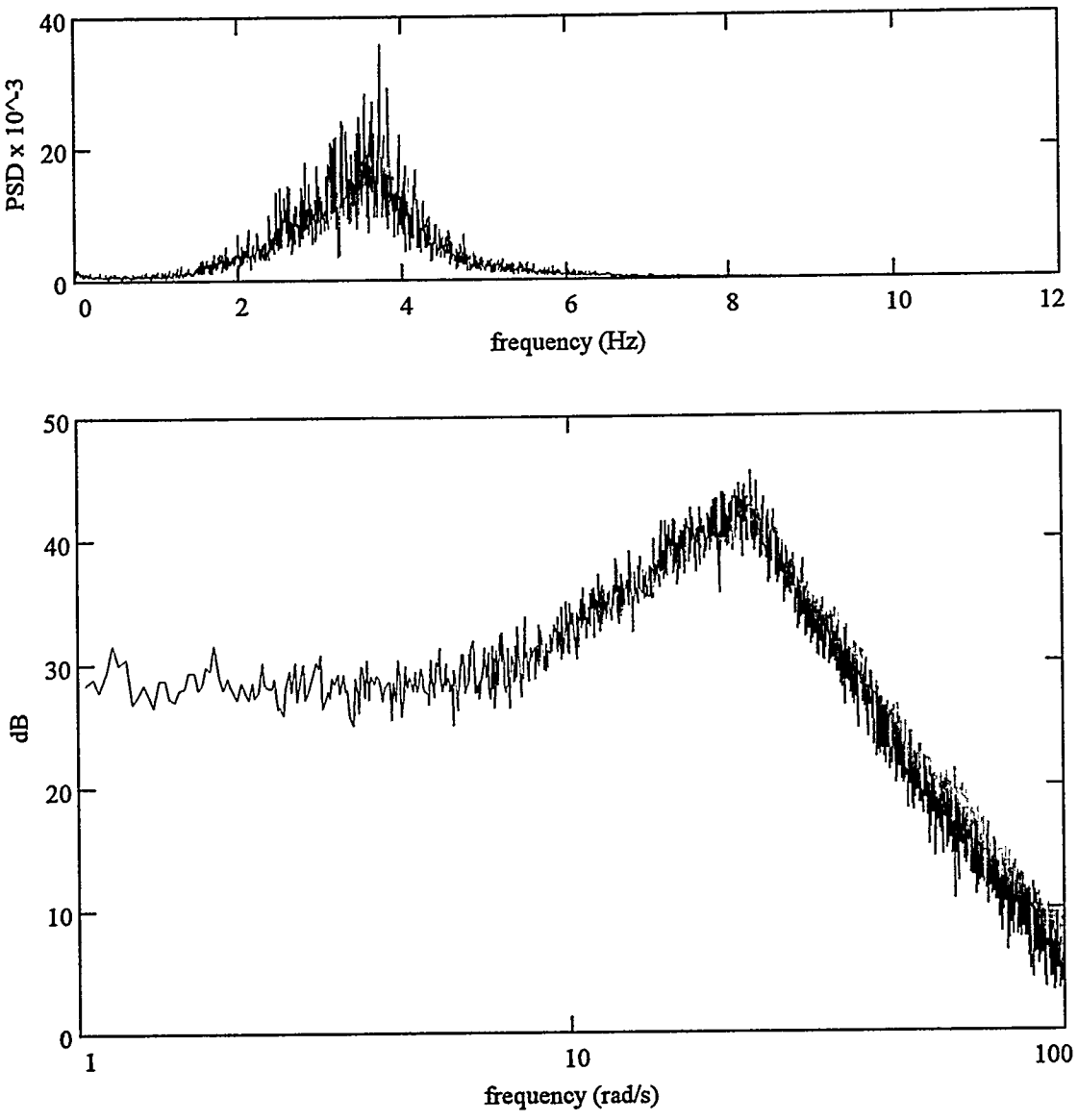

Figure 17: PSD and Bode plot of BFB fluctuations with 36 hole distributor

Experimental operating conditions			
Bed diameter	10.16 ± 0.01 cm	Bed height	10.0 ± 0.2 cm
Particle diameter	0.40 ± 0.01 mm	Pressure measurement	differential
Particle density	2600 ± 100 kg/m^3	Pressure tap position	Lower - 2.5 cm/Upper - 7.6 cm
Gas density (air)	1.20 ± 0.04 kg/m^3	Avg. voidage bwt. taps	0.50 ± 0.06
Superficial velocity	19.6 ± 0.6 cm/s ($U/U_{mf} = 1.4$)	Experiment number	7-3-1995-8.4

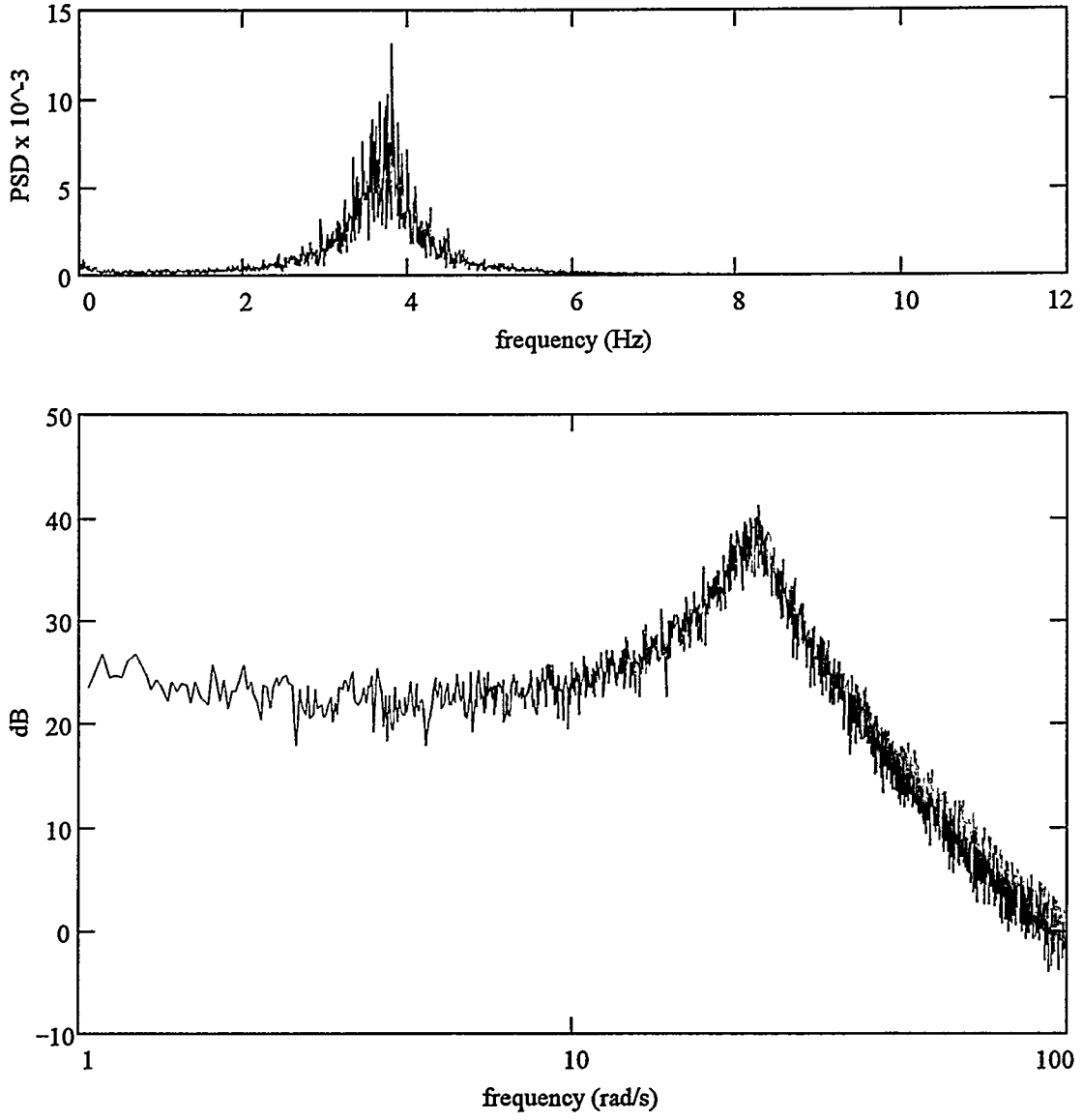

Figure 18: PSD and Bode plot of BFB fluctuations with 72 hole distributor plate

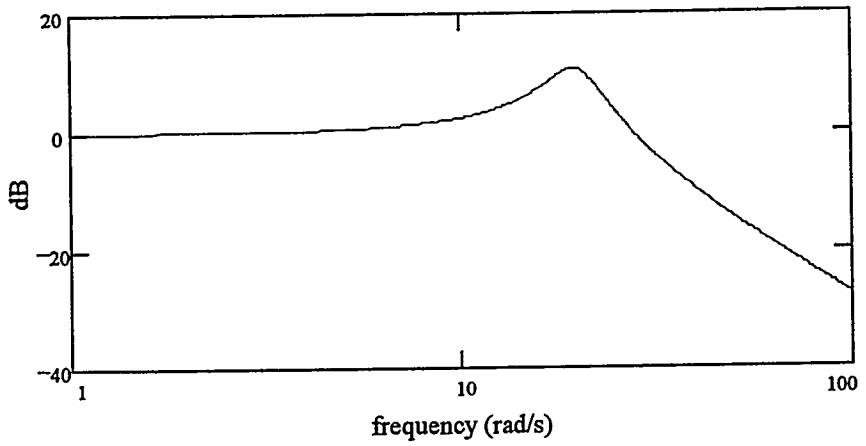

Figure 19: Example - simple 2nd order underdamped system Bode plot (ω_n=20 s^{-1}, ς=0.3)

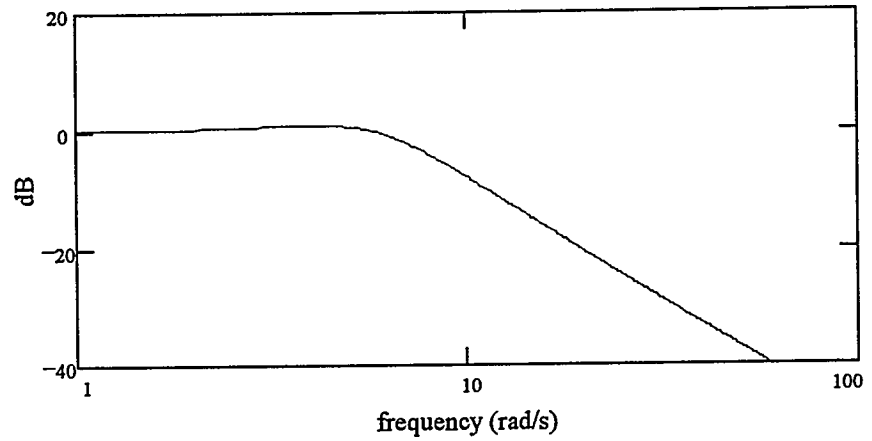

Figure 20: Example - simple 2nd order overdamped system Bode plot (ω_n=6 s^{-1}, ς=1.1)

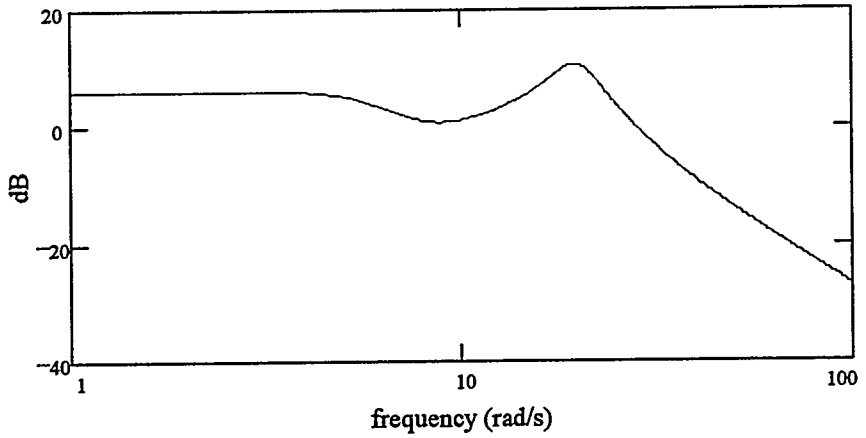

Figure 21: Example - Bode plot of the above second order systems acting in parallel

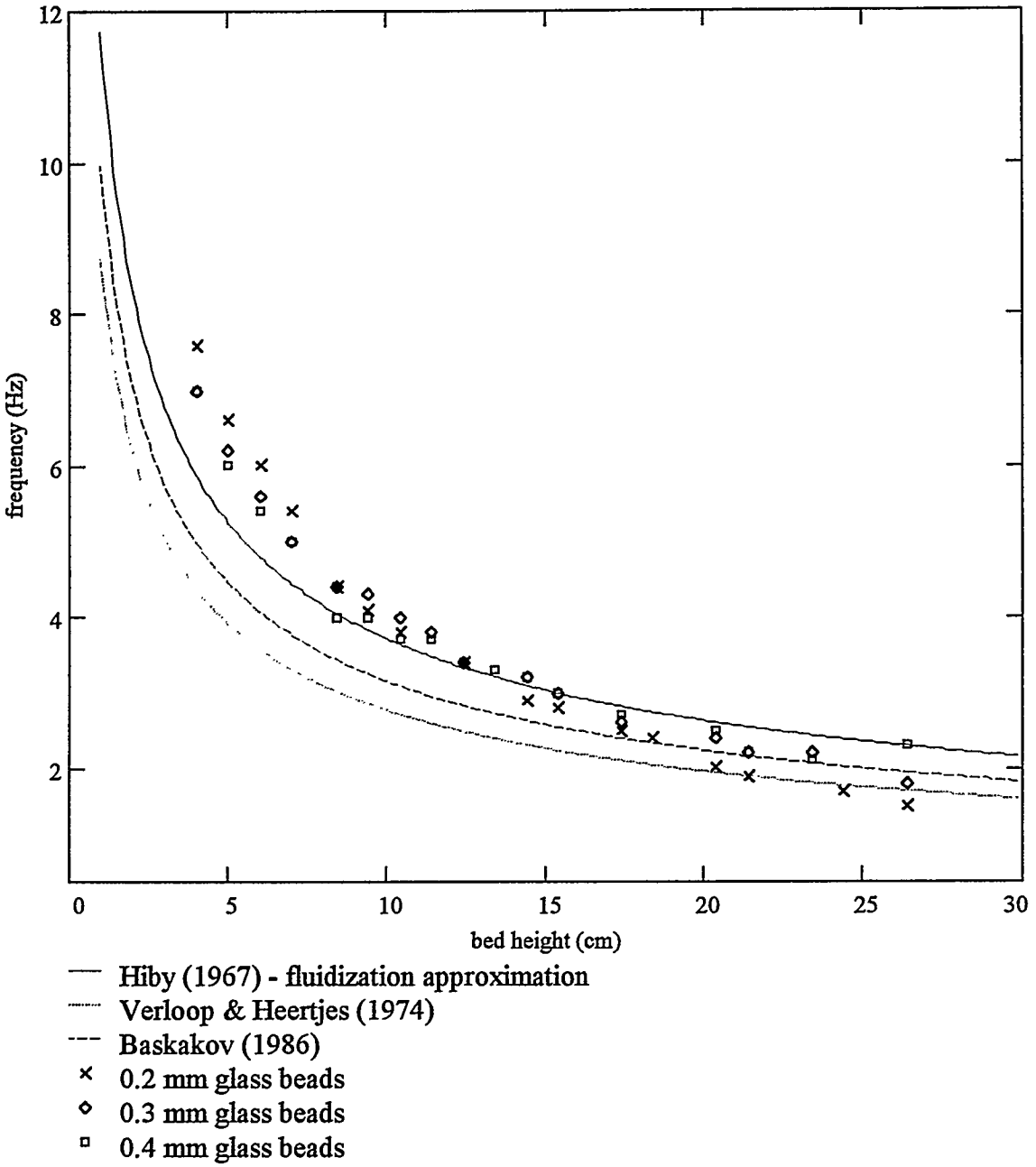

Figure 22: Comparison of proposed models to experimental data (D = 4.0")
Frequency vs. only the lowest dominant BFB frequency observed

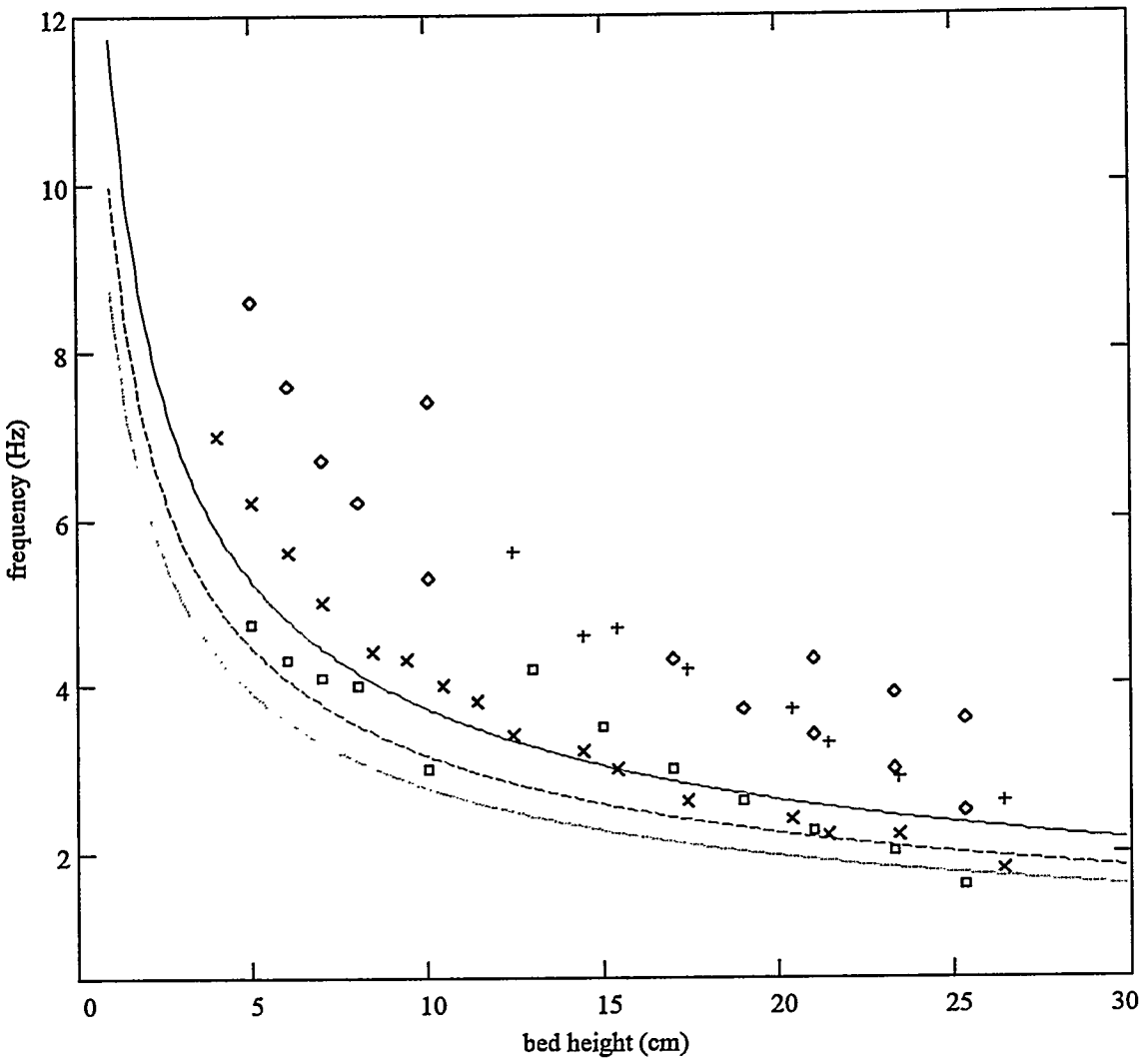

Figure 23: Comparison of proposed models to experimental data for 0.3 mm glass beads Frequency vs. all dominant BFB frequencies

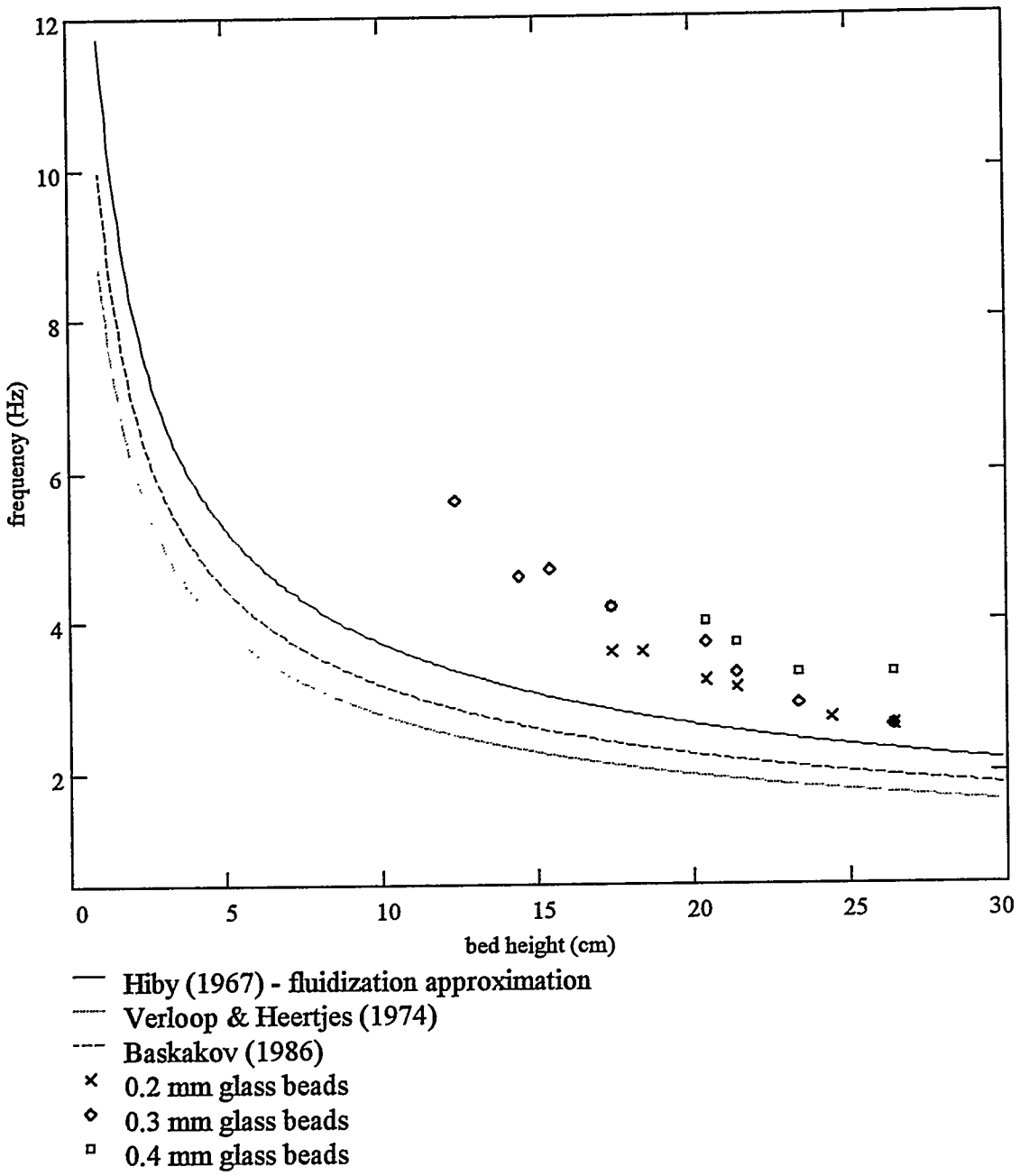

Figure 24: Comparison of proposed models to experimental data (D = 4.0")
Frequency vs. only the higher dominant BFB frequency observed

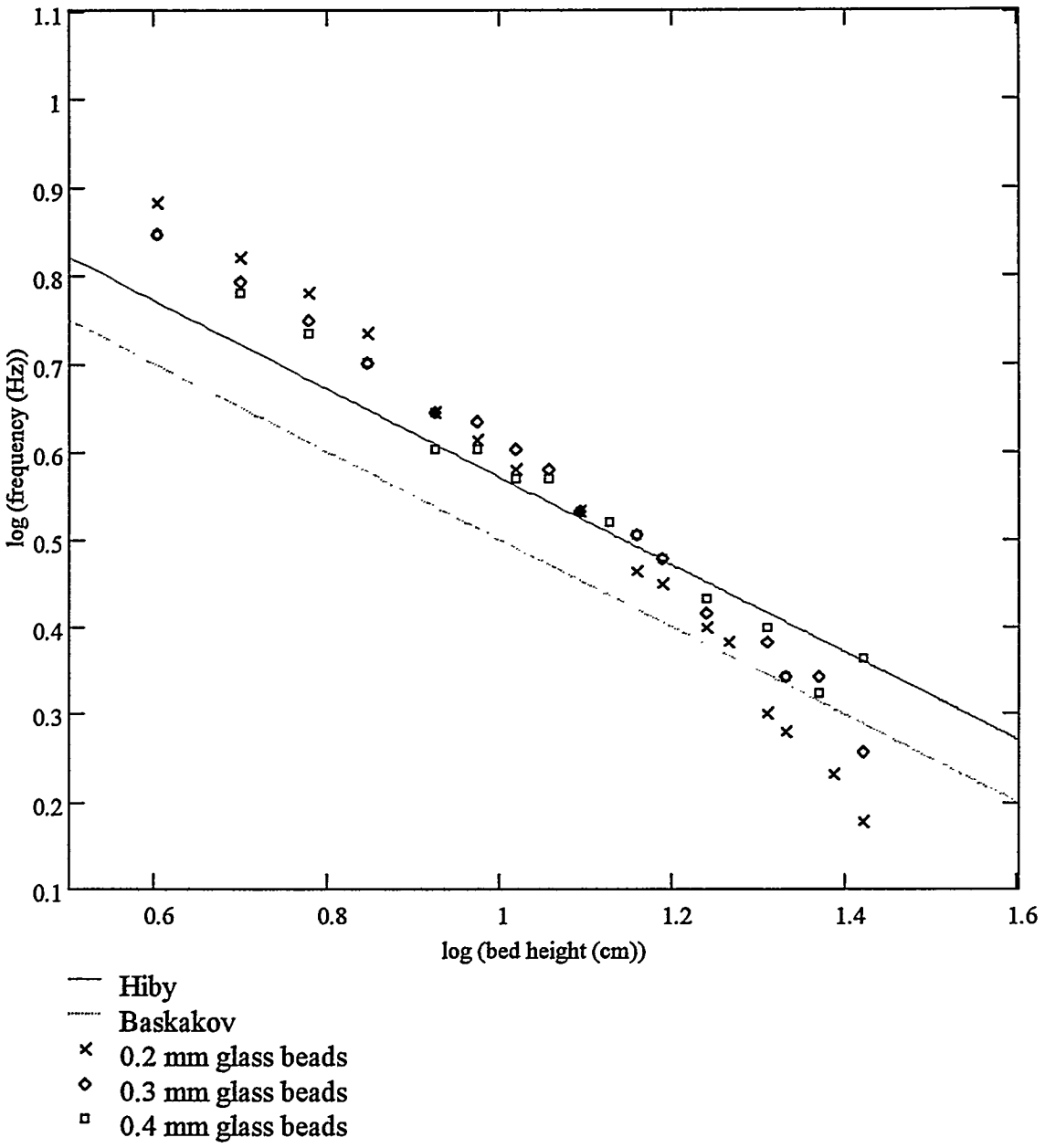

Figure 25: log-log comparison of proposed models to experimental data (D = 4.0")
log(frequency) vs. log(only the lowest dominant BFB frequency observed)

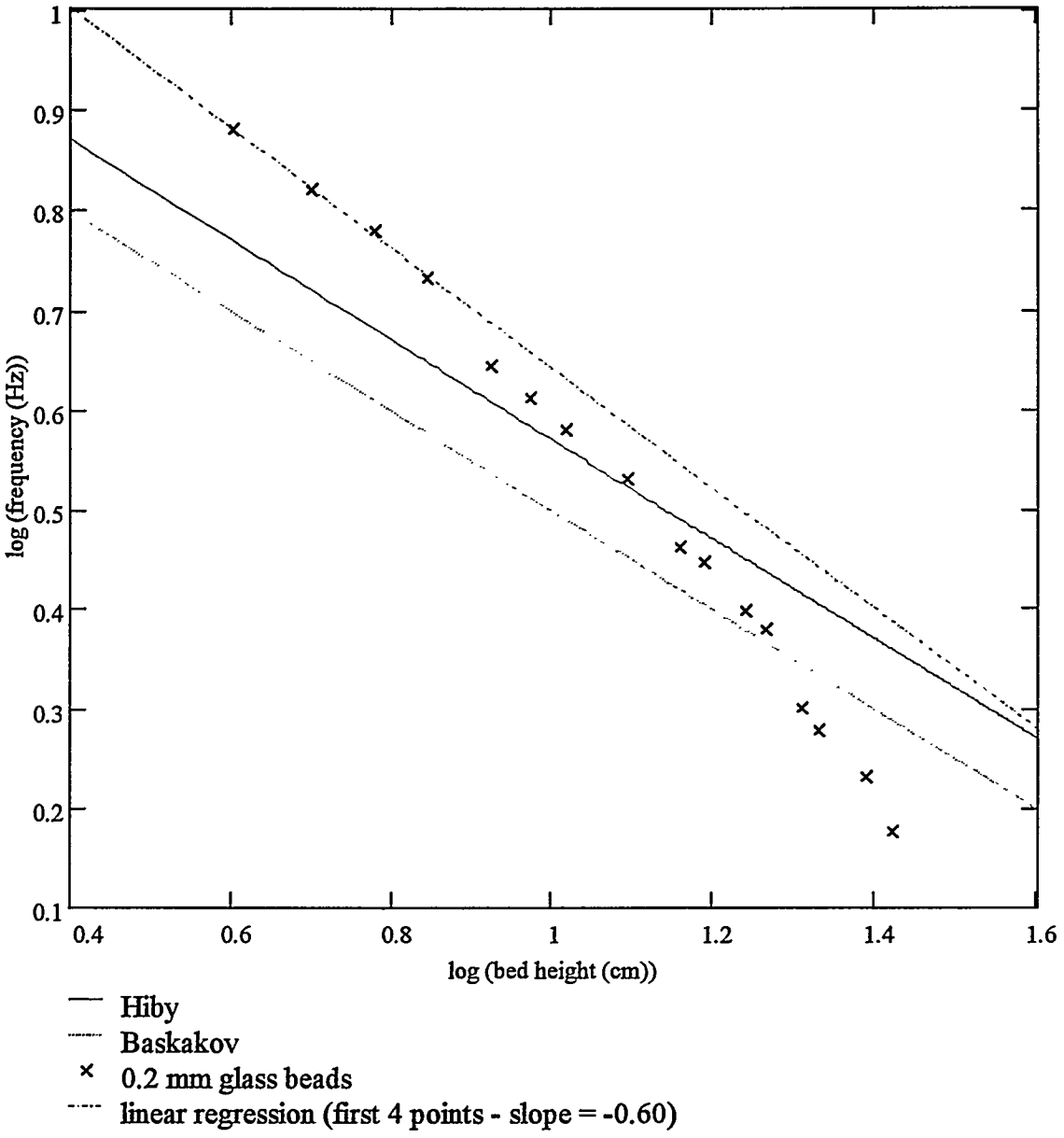

Figure 26: log-log comparison of proposed models to experimental data (D = 4.0") log(frequency) vs. log(only the lowest dominant BFB frequency observed) with linear regression of the first four data points of dp = 0.2 mm

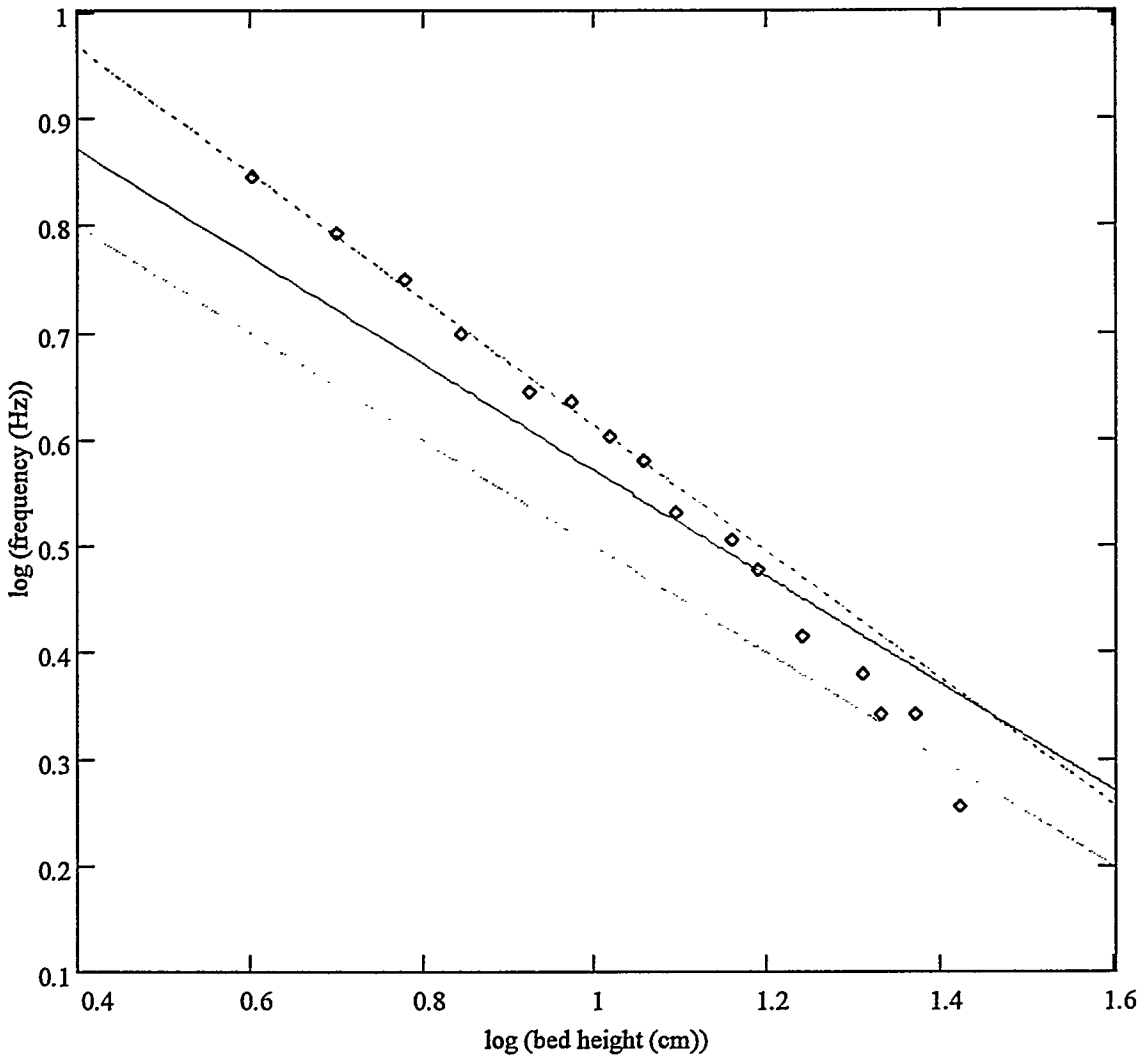

Figure 27: log-log comparison of proposed models to experimental data (D = 4.0")
log(frequency) vs. log(only the lowest dominant BFB frequency observed)
with linear regression of the first eight data points of dp = 0.3 mm

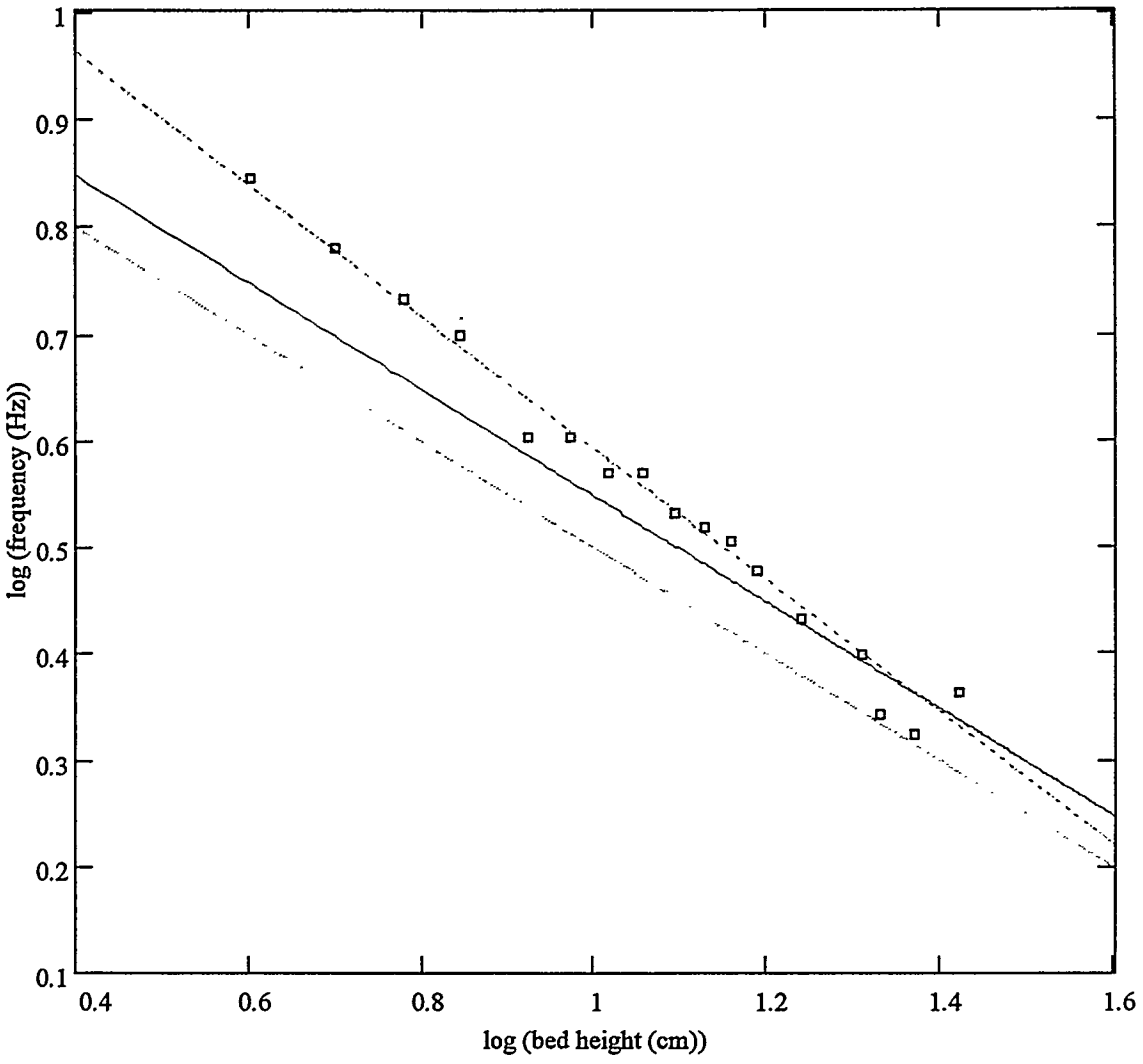

Figure 28: log-log comparison of proposed models to experimental data (D = 4.0") log(frequency) vs. log(only the lowest dominant BFB frequency observed) with linear regression of the first twelve data points of dp = 0.4 mm

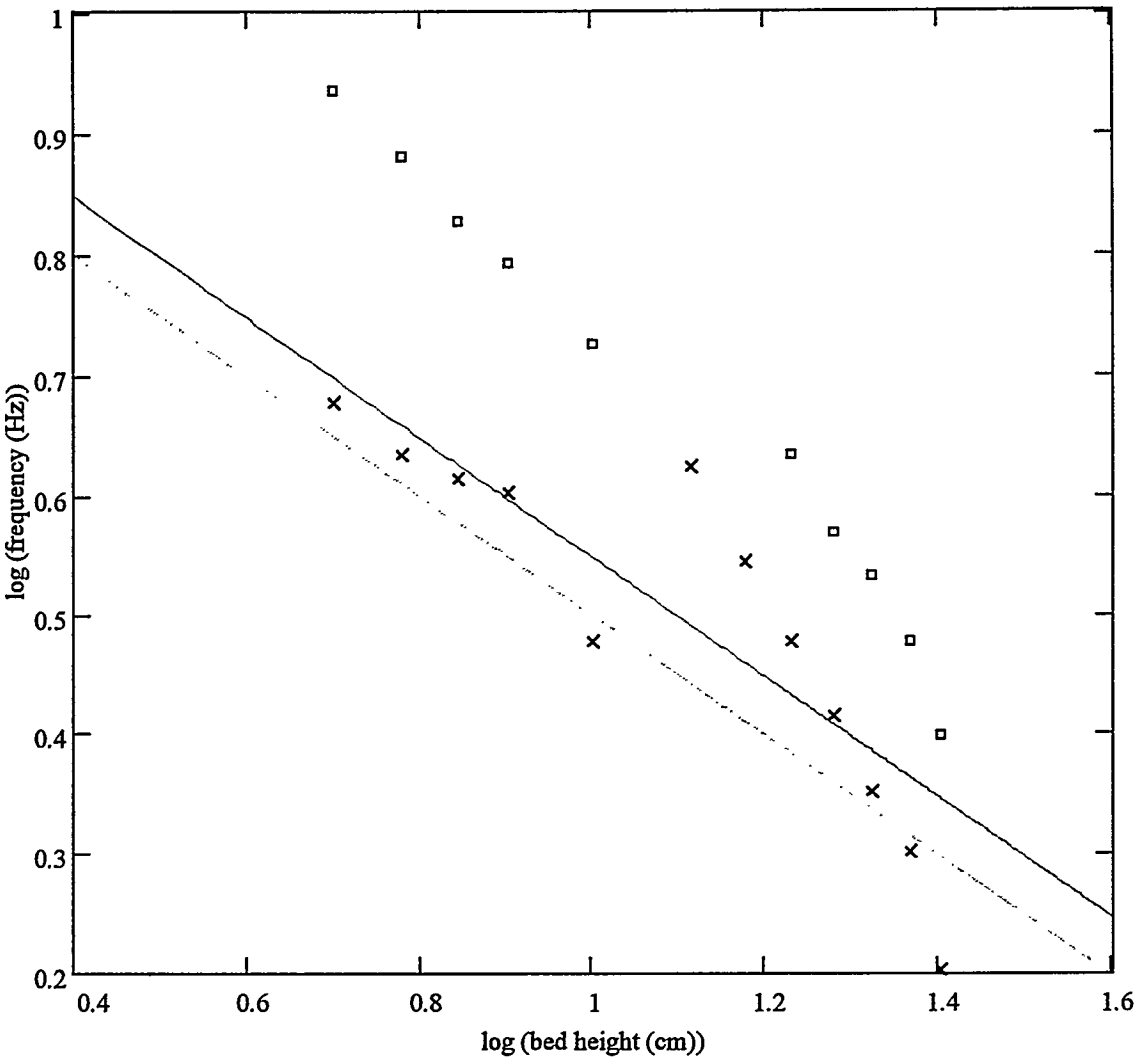

Figure 29: log-log comparison of proposed models to experimental data (D = 2.0") log(frequency) vs. log(all dominant BFB frequencies observed)

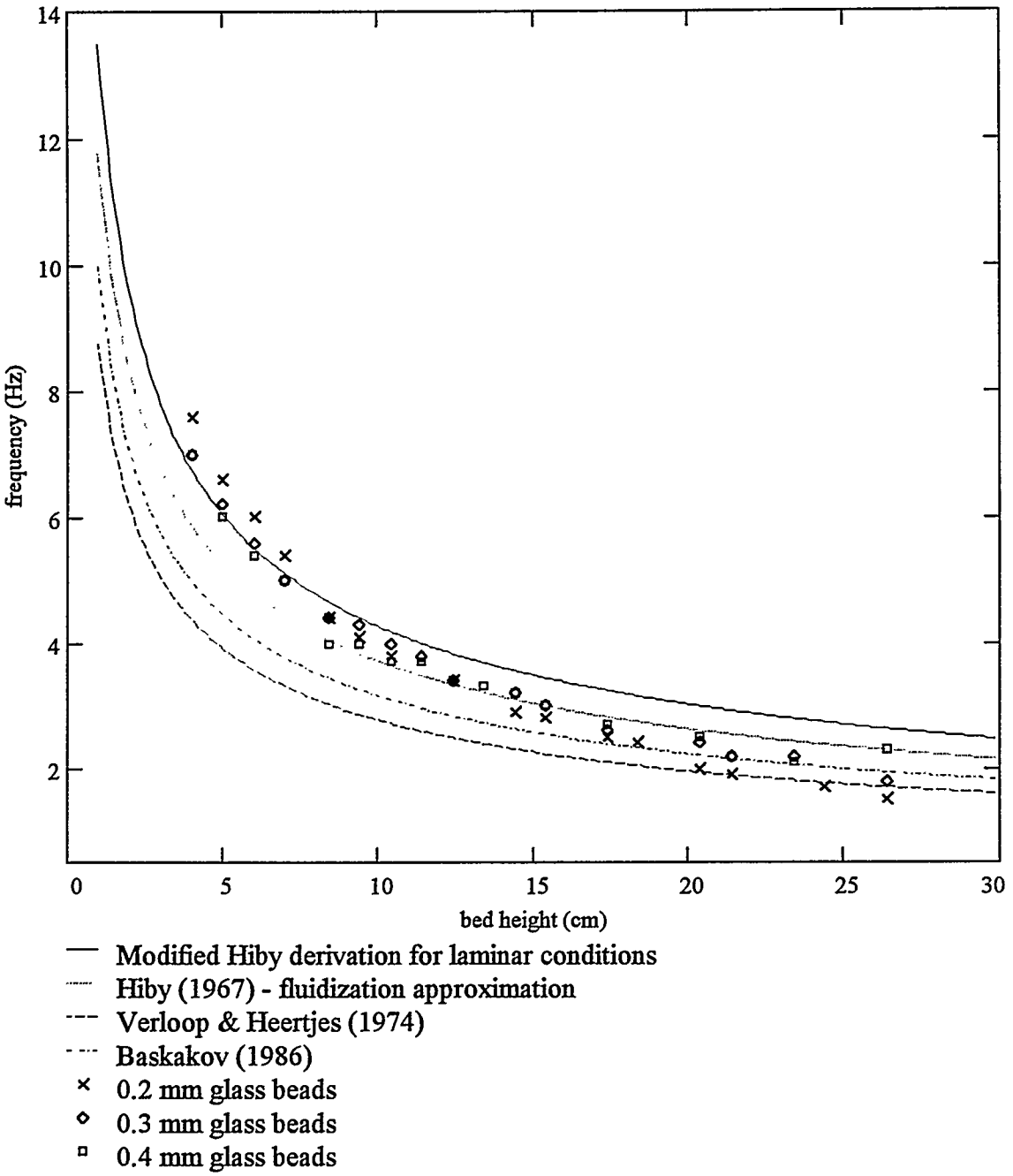

Figure 30: Comparison of modified Hiby model to experimental data (D = 4.0")
Frequency vs. only the lowest dominant BFB frequency observed

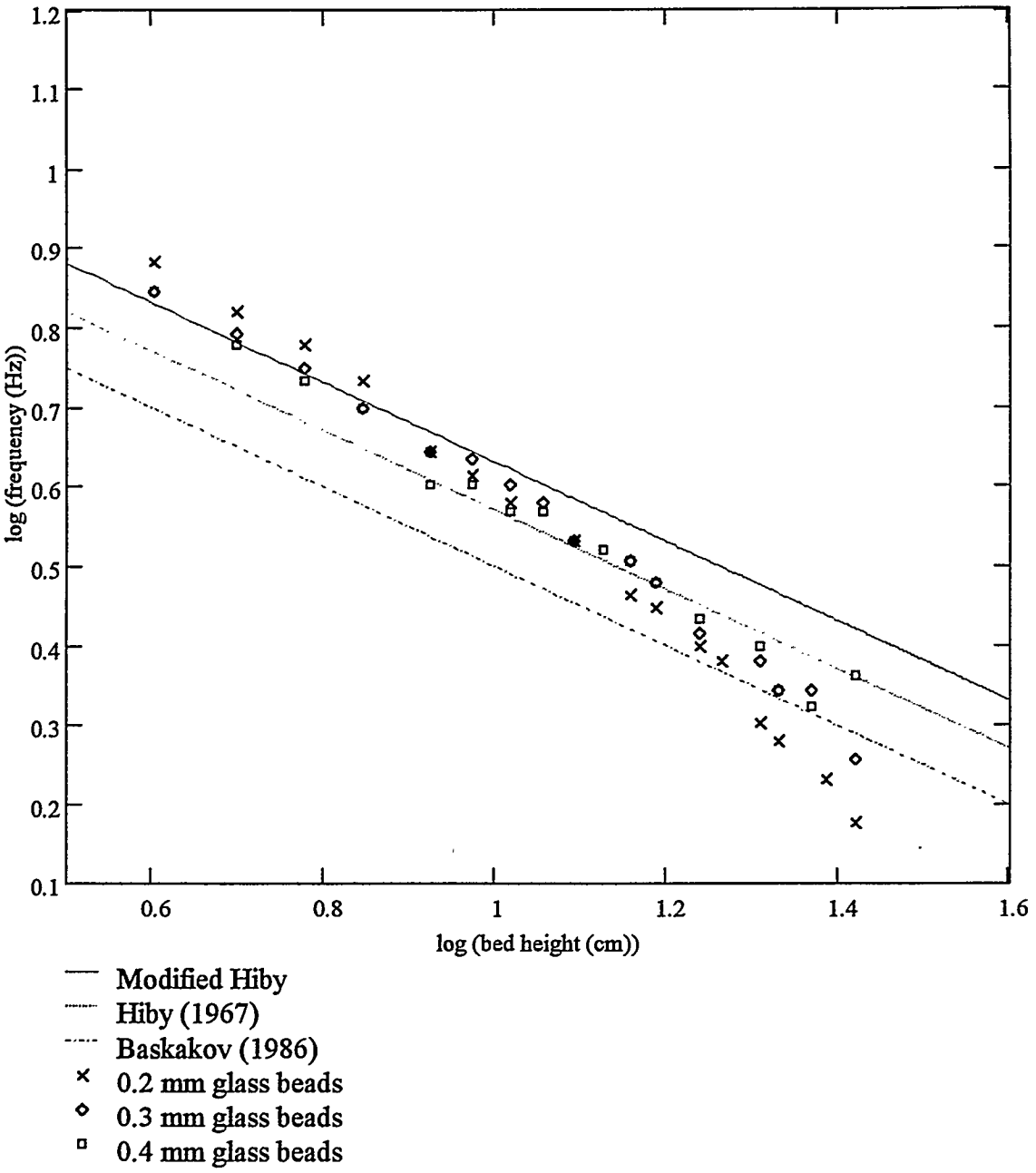

Figure 31: log-log comparison of modified Hiby model to experimental data (D = 4.0")
log(frequency) vs. log(only the lowest dominant BFB frequency observed)